NITROGEN CONTROLS ON CARBON AND WATER EXCHANGES

ANALYSIS OF NITROGEN CONTROLS

ON

CARBON AND WATER EXCHANGES IN A CONIFER FOREST

USING CLASS-CTEM^{N+} MODEL

By

SUO HUANG, B.Sc.

A Thesis

Submitted to the School of Graduate Studies

In Partial Fulfillment of the Requirements

For the Degree

Master of Science

McMaster University

MASTER OF SCIENCE (2009)   McMaster University
(Geography)   Hamilton, Ontario

TITLE: Analysis of nitrogen controls on carbon and water exchanges
                in a conifer forest using CLASS-CTEM^{N+} model

AUTHOR: Suo Huang, B.Sc.

SUPERVISOR: Professor M. Altaf Arain

NUMBER OF PAGES: ix, 57

ABSTRACT

Nitrogen (N) controls on carbon and water exchanges were analyzed in a 70-year old eastern temperate conifer forest in Ontario, Canada from 2003 to 2007 using a newly developed nitrogen (N) cycle coupled model -- CLASS-CTEM^{N+}. This process-based model incorporates sunlit and shaded big-leaves for C3 and C4 photosynthesis and semi-mechanistic canopy conductance formulation for dynamic plant-functional-types. Recently, key soil and plant N cycling algorithms have also been included (e.g., biological fixation, atmospheric N deposition, fertilization, mineralization, nitrification, denitrification, leaching, soil nitrous dioxide (N_2O) emissions, root N uptake, plant N allocation and N controls on plant photosynthesis capacity). The simulated values of soil-plant N contents and processes rates including N_2O fluxes were generally in agreement with observations.

Comparison of default non-N and C&N-coupled model simulations clearly revealed N controls on photosynthetic uptake and water loss. Predictions of daily gross ecosystem productivity (GEP), ecosystem respiration (R_e), net ecosystem productivity (NEP) and evapotranspiration (ET) showed better agreement with eddy covariance (EC) flux measurements when using the N-coupled model (RMSE of 1.97, 0.73, 1.44, 0.92; and MAE of 1.48, 0.55, 1.01, 0.60 for GEP, R_e NEP, and ET, respectively; n=1825) as compared to the non-N model simulations (RMSE of 2.95, 1.35, 1.93, 1.03; MAE of 2.38, 1.15, 1.55, 0.71 for GEP, R_e, NEP, and ET, respectively; n=1825) over 5 years (2003-2007). Annual values of N-coupled model simulated NEP were 134, 195, 183, 225 and 255 g C m^{-2} yr^{-1} for 2003-2007, as compared to non-N model simulated annual NEP values, which were 535, 562, 507, 540, and 535 g C m^{-2} yr^{-1} for respective years. These values

were compared to measured NEP values of 220±67, 126±67, 33±67, 142±67 and 102±67 g C m^{-2} yr^{-1} for the years 2003-2007, respectively. The difference between N-coupled model simulated and EC measured annual variations of carbon exchanges was largely due to specific extreme weather events (e.g. drought, spring warming) during certain years. Overall, the impacts of N limitations on carbon fluxes were more pronounced during early spring, late autumn and winter seasons. This newly developed model will help to evaluate the response of terrestrial vegetation ecosystems to N variations under different scenarios for future climate change.

ACKNOWLEDGEMENTS

TABLE OF CONTENTS

LIST OF FIGURES

LIST OF TABLES

CHAPTER 1: INTRODUCTION

The emission rates of greenhouse gases (GHGs) have rapidly increased in recent decades (IPCC, 2007). For example, carbon dioxide (CO_2) emission rate has increased from 1.3% per year in the 1990s to 3.3% per year during 2000 to 2006. Meanwhile, atmospheric nitrous oxide (N_2O), which has a residence time of 120 years and global warming potential (GWP) 320 times larger than CO_2, has increased by 18% since the middle of the eighteenth century. Overall N_2O is responsible for about 5% of total atmospheric warming and would have greater impact on warming in the future due to its increasing rate and largely unknown sinks (IPCC, 2007).

There is large uncertainty about the responses and feedbacks of Earth's terrestrial ecosystems to future climate change (Bonan, 2008; Ciais et al., 2005; Davidson and Janssens, 2006; Heimann and Reichstein, 2008; Scheffer et al., 2009). We do not fully understand how plant photosynthesis and evapotranspiration would be affected by higher atmospheric CO_2 concentrations in the future. This includes such questions as the potential of a so-called CO_2 fertilization effect (Oechel et al., 1994). Particularly in forest ecosystems where N is often limited, at least in terms of net carbon uptake (Vitousek and Howarth, 1991), it is not known how soil nitrogen availability would be affected by warmer temperatures and what would its impact would be on the strengths of terrestrial carbon sinks and source (Reay et al., 2008). N is an important nutrient for terrestrial ecosystems because it affects plant growth and thus vegetation cover, density and phenology (Hungate et al., 2003; Nadelhoffer et al., 1999; Schlesinger and Lichter, 2001). Many of the N-cycle processes and feedbacks are not fully understood. Experimental studies show that leaf nitrogen content has a strong

influence on photosynthesis, which partially controls stomatal conductance and hence evapotranspiration and energy balance (Dickinson et al., 2002; Schulze, 2000). Understanding N exchange processes is crucial to fully predicting the impact of human-induced N deposition and N fertilization on terrestrial vegetated ecosystems.

Some climate models have predicted that future climate warming will turn terrestrial ecosystems into carbon sources via a positive carbon-climate feedback scenario (Cox et al., 2000; Dufresne et al., 2002; Friedlingstein et al., 2006). Models included in the Fourth Assessment Report (AR4) of the IPCC also concluded that warming will increase atmospheric CO_2 emissions from terrestrial ecosystems (IPCC, 2007). However, most of these models had not fully considered the role of nutrient cycling and feedbacks, particularly N feedbacks. In recent years, some ecosystem models have evaluated N impacts on ecosystem functioning and responses by coupling C and N exchange processes (Sokolov et al., 2008; Thornton et al., 2007; Thornton et al., 2009). Thornton et al. (2007) reported that the inclusion of N-cycle in their model reduced the land carbon uptake under the rising CO_2 concentration by a factor of 3.8 by 2100, while it also reduced the terrestrial carbon cycle's sensitivity to changes in temperature and precipitation.

Forests are one of the most important terrestrial ecosystems and any changes in the functioning of forests would exert severe impact on the global carbon cycle and hence, global climate (Schimel et al., 2001). Many boreal and temperate forests are nitrogen-limited (Aber et al., 1998; Vitousek and Howarth, 1991), which impacts their growth and long-term survival. There is an urgent need to improve our understanding of the responses of forest ecosystems to climate

change by using ecosystem models in which the physical, biological, and biogeochemical processes are dynamically coupled.

In this study, a newly developed carbon and nitrogen coupled model, the Canadian Land Surface Scheme - Canada Terrestrial Ecosystem Model (CLASS-CTEM^{N+}) was used to study plant and soil nitrogen processes and their impacts on carbon and water exchanges in a 70-year old eastern temperate conifer forest in Canada over five years (2003-2007). Observed data used in this study included: energy, CO_2 and water vapour fluxes from eddy covariance operation, N_2O fluxes from closed-chambers and soil-plant N variables derived in field and laboratory studies. The objectives of this study were: (1) to develop the next-generation of Canadian Terrestrial Ecosystem Model (CTEM) for Canadian Global Climate Model (GCM), by implementing soil-plant N cycling processes; (2) to evaluate the model's capability in simulating soil-plant N processes in a temperate conifer forest ecosystem; (3) to analyze N impacts and controls on carbon and water exchanges in this forest; and (4) to determine the sensitivity of model's responses to climate variability and natural/anthropogenic effects. The newly developed model would help to improve our understanding of carbon, water and nitrogen cycle dynamics in forest ecosystems and explore the ability of the model in predicting coupled carbon and nitrogen exchanges under future climate change.

CHAPTER 2: MATERIALS AND METHODS

2.1 Model description

The CLASS-CTEM^{N+} model was developed by incorporating soil and plant nitrogen cycling algorithms acquired from Arain et al. (2006) and Dickinson et al. (2002) in the Canadian Land Surface Scheme (CLASS; Verseghy, 1991; Verseghy et al., 1993) and the Canadian Terrestrial Ecosystem model (CTEM; Arora and Boer, 2003; Arora and Boer, 2005a, b; Arora and Boer, 2006). Soil N_2O emissions were also included in the model following Firestone and Davidson (1989) and Parton et al. (1996). The soil and plant N algorithms were converted into a daily time step to be compatible with the CTEM time step. CLASS was originally developed to provide land-surface processes such as energy and water exchanges; and CTEM was developed to provide photosynthesis, canopy conductance, autotrophic and heterotrophic respiration, carbon allocation and structural attribution, phenology, turnover, mortality, disturbances, and vegetation competition in the Canadian General Circulation Model (CGCM). Apart from coupled CGCM studies, CLASS and/or CTEM models have been extensively used for site-specific and synthesis studies to simulate energy, water and carbon exchanges in various terrestrial ecosystems (Arain et al., 2002; Arain et al., 2006; Arora, 2003; Grant et al., 2005; Grant et al., 2006; Kothavala et al., 2005; Wang et al., 2001; Yuan et al., 2007).

A schematic of the key CLASS-CTEM^{N+} processes is shown in Fig. 1. It includes four nitrogen pools i.e., leaf, stem, root and non-structural reservoir. Simulated soil and plant N processes are connected by demand and supply of respective N pools.

4
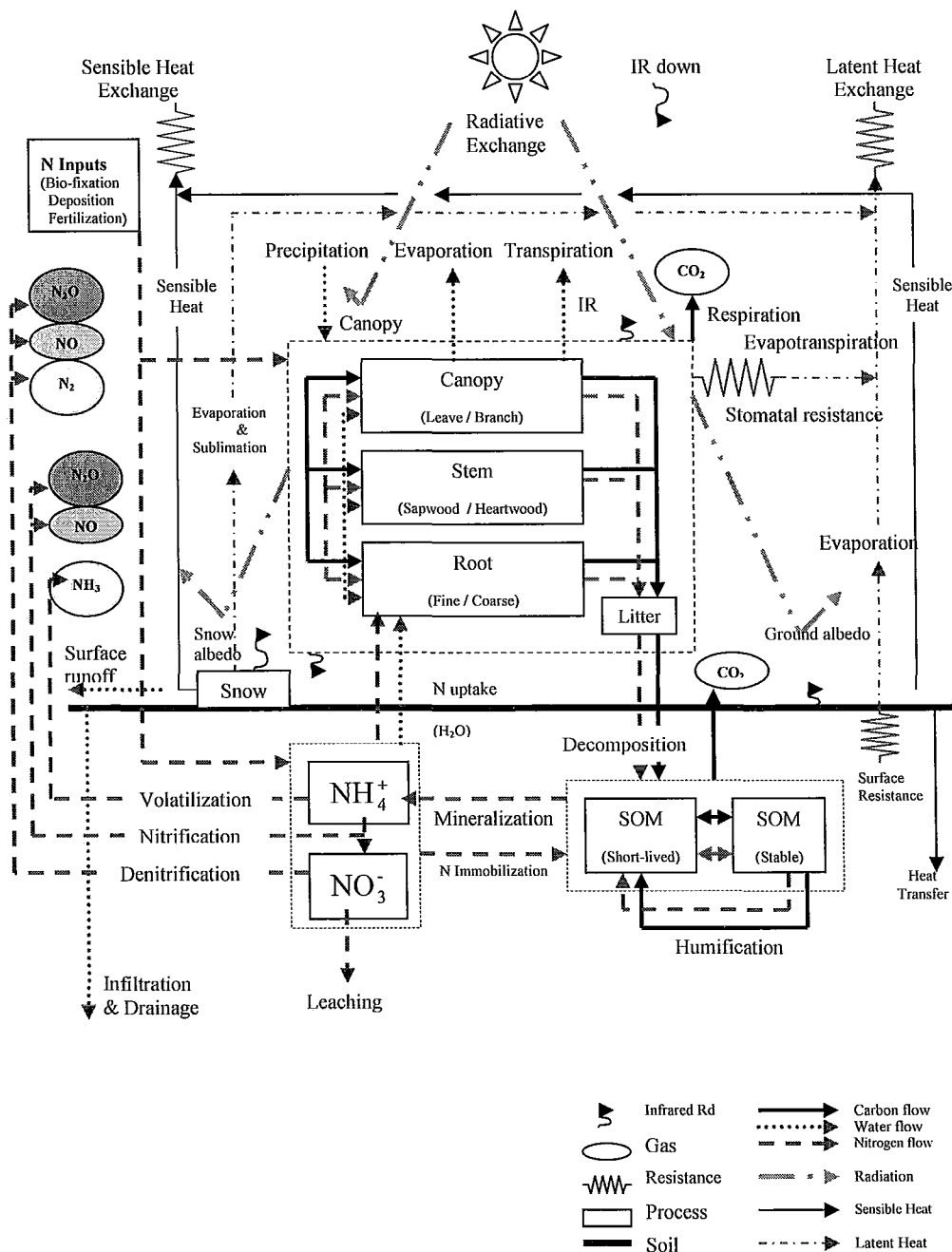
Figure 1: Schematic representation of CLASS-CTEM^{N+} model processes.

2.1.1 Soil N processes

Soil N-cycle processes in CLASS-CTEM^{N+} include N immobilization, N mineralization, nitrification, denitrification, volatilization, leaching, disturbance losses, and soil trace gas (N_2O) fluxes.

Because organic N in soil organic matter (SOM) pools generally does not escape from the soil system, decomposition tends to enrich N concentration in SOM pools over longer time scales. The fraction of litter N being transformed into short-lived and stable SOM is about 40% and 60%, respectively, of total decomposable litter N. In order to stabilize the N:C ratio in the stable SOM pool, N transformation from stable to short-lived SOM (humification) is estimated as:

$$K_{hum} = (R_{ssom} + C_{som-->fom}) \cdot NC_{som} \tag{1}$$

where, R_{ssom} is the C releases to the atmosphere, and $C_{som->fom}$ is the C releases from the short-lived and stable SOM, with a N:C ratio of NC_{som}.

Even though decomposition of stable SOM pools can produce inorganic N, it is appropriate to assume that all the production of inorganic N mainly comes from the short-lived SOM pool, because the latter involves soil biota and mineralizable forms of SOM, including those from decomposition of stable SOM. Therefore the N mineralization and feedback due to higher inorganic-nitrogen (immobilization) may be simplified as:

$$K_{\min} = R_{sfom} \cdot NC_{fom} \cdot \exp(-0.05 / NC_{fom}) \tag{2}$$

where R_{sfom} and NC_{fom} represent short-lived SOM respiration and actual N:C ratio with a threshold N:C ratio value of 0.05 below which immobilization by bacteria takes place.

Nitrification is the conversion of NH_4^+ to nitrate (NO_3^-) in the soil, during which autotrophic nitrifiers use the energy yield from NH_4^+ oxidation to fix carbon used in growth and maintenance while heterotrophic nitrifiers gain their energy from breakdown of organic matter (Chapin et al., 2002) (Fig. 1). The microbes involved in these activities are sensitive to soil temperature, soil moisture, pH value and NH_4^+ concentration. The rate of microbial activity is important and leads to secondary emissions of NO and N_2O. Soil water levels, soil temperature effects and NH_4^+ concentrations are implicitly related to calculate nitrification rate (Dickinson et al., 2002):

$$K_{nit} = [K_{ni0} \cdot f(T_{rt}) \cdot \frac{W_{rt}/\rho_{rt} \cdot (1 - W_{rt}/\rho_{rt})}{0.25 + 1/NH_4^+}] \cdot NH_4^+ \tag{3}$$

where k_{ni0} is a prescribed maximum nitrification rate, $f(T_{rt})$ is root zone Q_{10} temperature function. W_{rt} is the function of soil moisture dependence of nitrification and ρ_{rt} is the total root zone porosity. If the soil is very wet or if there is leaching from the soil system through drainage, accumulated nitrate (NO_3^-) ions in the soil could be released into the air through denitrification. In this process, NO_3^- is converted to NO_2^-, NO, N_2O and N_2 (Fig. 1), which may be influenced by soil temperature, soil pH, and N content:

$$K_{dent} = k_{dn0} \cdot (\frac{W_{rt}}{\rho_{rt}})^B \cdot f(T_{rt}) \tag{4}$$

where k_{dn0} is maximum denitrification rate, $f(T_{rt})$ is root zone temperature function, W_{rt} is root zone soil moisture, ρ_{rt} is root zone porosity, and B is the Clapp-Hornberger parameter.

In CLASS-CTEM^{N+} we also added processes simulating soil nitrogen trace gas fluxes of nitrous oxide (N_2O). Factors controlling N_2O production include soil texture, pH, soil temperature, water-filled pore space (WFPS), soil respiration and NH_4^+ concentration (Parton et al., 1996):

$$Nitr^{N_2O} = f(WFPS) \cdot f(pH) \cdot f(Trt) \cdot (K_{max} + N_{max} \cdot f(NH_4^+)) \tag{5}$$

where $f(WFPS)$ is the water-filled pore space (WFPS) nitrification function:

$$f(WFPS) = (\frac{WFPS - Nb}{Na - Nb})^{Nd \cdot (\frac{Nb-Na}{Na-Nc})} \cdot (\frac{WFPS - Nc}{Na - Nc})^{Nd} \tag{6}$$

where Na, Nb, Nc, Nd are the parameters of WFPS for nitrification, prescribed in the model as 0.55, 1.70, -0.007 and 3.22, respectively. $f(pH)$ is the effect of soil pH on nitrification fraction, $f(T_{rt})$ is root zone temperature function, $f(NH_4^+)$ is the effect of soil ammonium level on nitrification fraction. K_{max} is the parameter for N turnover coefficient, and is assumed to be proportional to the soil N turnover rate, which is a function of the soil texture, soil N fertility (or N fertilizer additions), and soil management practices. N_{max} is the maximum nitrification N_2O gas flux (30 g N ha^{-1} d^{-1}) with excess soil NH_4^+. Once this process is completed, soil NH_4^+ concentration is updated, and a fraction of N is lost as gas in the model's soil N pools.

Along with denitrification, N_2 and N_2O emissions were produced together. Total N (N_2+N_2O) gas flux is estimated as (Parton et al., 1996):

$$Deni^{tot} = min(F_d(NO_3), F(CO_2))F_d(WFP) \tag{7}$$

where $Deni^{tot}$ is the total N_2 and N_2O gas emission from denitrification; $F_d(NO_3)$ and $F_d(CO_2)$ are the maximum total N gas flux for a given NO_3 and soil respiration rate, respectively; and $F_d(WFP)$ is the effect of water on denitrification.

N_2O from denitrification ($Deni^{N2O}$) was calculated as a fraction of produced total N_2 and N_2O gas as:

$$Deni^{N_2O} = \frac{Deni^{tot}}{(1 + R_{N_2/N_2O})} \tag{8}$$

Where $R_{N2/N2O}$ is the ratio of $N_2:N_2O$ during denitrification. Thus, the total N_2O from nitrification and denitrification in the soil was added by eq. 5 and eq. 8.

And N_2 emission is calculated in the similar way:

$$Deni^{N_2} = \frac{Deni^{tot}}{(1 + 1/R_{N_2/N_2O})} \tag{9}$$

2.1.2 Plant N processes

Based on sunlit and shaded big-leaves submodels of photosynthesis and stomatal conductance for C3 and C4 differentiated dynamic plant-functional-types, plant N processes were incorporated in the model through root N uptake, plant N allocation and N controls on photosynthesis capacity. N uptake through roots is the main source of N supply (besides bio-fixation and atmospheric deposition into the ecosystem) and depends upon three processes: ion transport from the soil to the root surface, transport from the root surface to the root interior, and allocation into various N pools (sinks). Modeled root N uptake is determined by soil inorganic ion transportation at the root interface. Non-structural C pool increments are defined as a function of both leaf and fine root biomass C, with a range of prescribed C:N ratios for N storage (due to either reallocation or excess soil supply) or re-use (Arain et al., 2006). For plant N, the model uses dynamic maximum carboxylation capacity of Rubisco (V_{cmax}), which is determined nonlinearly from the modelled leaf Rubisco-nitrogen, using a relationship derived from Warren and Adams (2001). Hence, variations in plant carbon assimilation due to vertical changes in sunlit and shaded leaves, and thus stomatal conductance, are linked with leaf N status through Rubisco enzyme. The N uptake rate can be enhanced or limited by plant growth, depending on N demand and non-structural storage capacity. Detailed equations of plant N processes simulations are described in Arain et al., (2006) and Appendix A.

Apart from plant litter-fall, there are three other sources of inorganic N additions to the soil-plant ecosystem (Fig. 1): (i) bio-fixation input as a function of vegetation coverage, excess soil nitrate, plant structural C pools and environmental temperature; (ii) prescribed atmospheric deposition, including both wet and dry depositions; (iii) nitrogen fertilization (organic or inorganic). Nitrogen losses included leaching and drainage, N gaseous emissions (currently including NH_3, N_2 and N_2O fluxes), and N disturbance losses (e.g. fire, harvest, runoff). After an update of sources and losses, soil NH_4^+ and NO_3^- ion availability for plant root uptake were passed to the next time step. Further details of soil-plant nitrogen processes simulations are given in Appendix A.

2.2 Site and observed data description

The study site (42.7122° N, 80.3572° W) is located about 12 km south of the town of Simcoe, near Lake Erie in Southern Ontario, Canada. The site is known as the Turkey Point 1939 plantation forest (TP39) or TP4 in global Fluxnet synthesis studies and is part of the Canadian Carbon Program (CCP) or previously the Fluxnet-Canada Research Network. It is a mono-culture white pine (*Pinus strobus* L.; a drought-resistant species) forest. Mean tree height is 21.8±1.7 m (measured in 2007), mean tree diameter at DBH is 35.5±5.9 cm, and tree density is 425±172 trees ha^{-1} (Peichl and Arain, 2006; Peichl and Arain, 2007).

Climate in this region is cool temperate, with an annual mean air temperature of 7.8 °C and annual mean precipitation of 1010 mm, with 133 mm falling as snow (based on a 30-year-record from Environment Canada). The mean annual frost-free period is 160 days, and mean length of the growing season is 212 days (Presant and Acton, 1984). The soil type is brunisolic grey brown luvisol, well-drained with a medium- to coarse-grained sandy soil texture.

Shortwave and longwave radiations, wind speed and direction, air temperature, relative humidity (at 28 m), precipitation above tree height, and snow-depth were measured following Fluxnet-Canada protocols (Fluxnet-Canada, 2004; Arain and Restrepo-Coupe, 2005). Half-hourly fluxes of CO_2, water vapor and energy were also continuously measured since 2002 using a closed-path eddy covariance (EC) system mounted on top of a 28-m high scaffolding tower (Arain and Restrepo-Coupe, 2005). N_2O flux measurements were conducted using closed chambers, while soil NH_4^+ and NO_3^- concentrations, mineralization and nitrification rates, were measured using the buried-bag incubation at monthly intervals during the growing seasons of 2006 and 2007 (Peichl et al., 2009a).

Meteorological conditions from 2003 to 2007 are shown in Fig. 2. The study period recorded, on annual basis, warming trend as compared to the last 30-year mean air temperature of 7.8 °C. 2003 was the coldest year with annual air temperature of 7.39 °C. It also had the lowest average growing season temperature. A record and near-record warm spring and summer was observed in 2005 (Arain, 2009) and a warm winter and spring was observed in 2006, with the highest mean annual temperature of 9.74 °C among the 5 years. The highest annual average specific humidity value of 7.15 (g Kg^{-1}) was observed in 2005, while the lowest annual average specific humidity of 6.43 g Kg^{-1} was occurred in 2003. The site experienced the wettest year in 2006 with annual precipitations of 1187 mm, followed by 2004 and 2003, which received 935 and 913 mm, respectively. 2007 was a very dry year, with an annual precipitation of only 705 mm. 2005 had a spring and early summer drought (Arain, 2009) but its annual precipitation was near normal with an annual total value of 862 mm.
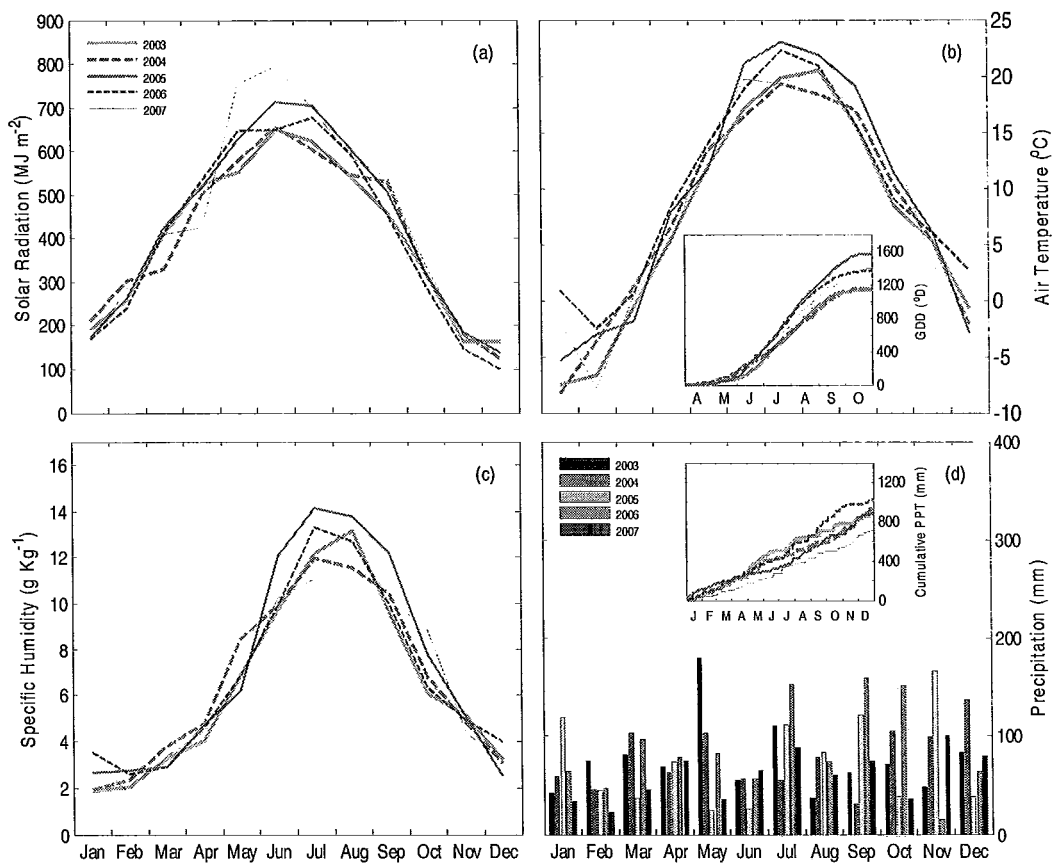
Figure 2: Monthly values of (a) solar radiation (MJ m^{-2}), (b) mean air temperature (°C) and growing season (Apr.-Oct.) degree days (GDD, shown in inset), (c) specific humidity (g Kg^{-1}), and (d) precipitation (mm) and cumulative daily precipitation (mm, shown in inset) from 2003 to 2007.

2.3 Model initialization, parameterization and sensitivity test

Off-line model simulations were performed using observed half-hourly meteorological forcing data from 2003 to 2007, including downwelling shortwave and longwave radiation, air temperature, specific humidity, wind speed, atmospheric pressure and precipitation.

The model required initial values of vegetation characteristics, such as initial leaf area index (LAI), tree height, rooting depth and biomass, soil characteristics, soil temperature and soil water content. These values were specified based on field observations or general site knowledge (see Table. 1). Initial conditions for SOM were obtained from equilibrium runs. The model was spun-up for 15 years, using the same forcing data repetitively and resetting the aboveground biomass, litter and total carbon content in SOM each year to their observed values to stabilize aforementioned initial variables before starting formal simulations on January 1, 2003. For plant and soil N initializations, field measurements were used whenever available (Peichl et al., 2009a). No parameter adjustments were made to fit the model to observed flux data and default parameter values for coniferous forests were used in this study. Table 2 shows some of the key nitrogen parameters used to run the model at our site.

Sensitivity analyses were also performed to evaluate the CLASS-CTEM^{N+} model's response to the possible influences of climate variability and N changes. For climatic variables, the sensitivity was evaluated by increasing/decreasing half-hourly values of (i) incident solar radiation by -10%, -5%, 0%, +5%, +10% of observed value, as five levels of sensitivity test, (ii) air temperature by -1.0°C, -0.5°C, 0°C, +0.5°C and +1.0°C of observed value, (iii) precipitation by -20%, -

10%, 0%, +10% and +20% of observed values, and (iv) CO_2 concentration by -40, -20, 0, +20 and +40 ppm of the baseline value of 360 ppm, respectively. Sensitivity tests of N enrichment were conducted by increasing (i) N deposition rate to 1, 1.25, 1.5, 2.0 g N m^{-2} yr^{-1} from the current rate of 0.75 g N m^{-2} yr^{-1}; and (ii) simulating N fertilization applications at four levels (i.e. 1, 2 3, 5 g N m^{-2} yr^{-1}) based on the original benchmark value of zero (no fertilization applied); and (iii) by increasing litter N:C ratio by -20%, -10%, 0, +10% and +20% with benchmark value of 0.048. One variable was changed at a time, while all others were kept unchanged during the sensitivity runs. Impact of climate and N variations was mainly focused on the responses of carbon (i.e. gross ecosystem productivity, GEP; ecosystem respiration, R_e; net ecosystem productivity, NEP) and water exchanges (evapotranspiration, ET).

Table 1: Site characteristics

Description	Value
Maximum leaf area index (LAI) (m^2 m^{-2}) [a]	8.0
Leaf biomass (kg C m^{-2}) [b]	0.1
Stem biomass (kg C m^{-2}) [b]	7.3
Aboveground biomass (kg C m^{-2}) [b]	8.4
Root biomass (>2mm) (kg C m^{-2}) [c]	1.9
Forest floor (LFH) biomass (kg C/m^{-2}) [c]	1.2
Soil $pH_{(CaCl)}$ (0 – 10cm) [b]	4.1
Bulk density (0 – 10cm) (g cm^{-3}) [b]	1.35
Soil C (0-55cm) (kg C m^{-2}) [b]	3.7

[a] Chen et al. (2006);
[b] Peichl and Arain (2006);
[c] Peichl et al. (2009a); Peichl et al. (2009b); Peichl et al. (2009c).

Table 2: Nitrogen parameters used in this study

Parameters	Value
Canopy LAI Rubisco-N content (g N m^{-2} LAI) [a]	2.00
Canopy nitrogen content (dry leaf matter, g N 100g^{-1}) [b]	1.16
Canopy Rubisco-N decay coefficient [a]	0.55
Canopy nitrogen decay coefficient [a]	0.25
N:C ratio in leaves [a]	0.027
N:C ratio in stems [a]	0.002
N:C ratio in roots [a]	0.010
N:C ratio in litter [c]	0.048
N:C ratio in SOM [d]	0.035
Ideal structural N:C ratio for new leaves [a]	0.024
Ideal N:C ratio in new stem tissue [a]	0.002
Ideal N:C ratio in new root tissue [a]	0.015
K_{max}, N turnover coefficient [f]	20.0
N_{max}, Max. nitrification N$_2$O gas flux with excess soil NH$_4^+$ (g N ha^{-1} d^{-1})[f]	30.0
High affinity maximum rate of ion uptake (non-dimensional) [a]	1.0
Low affinity root ion uptake [a]	0.2
Solubility of NH$_4^+$ ion [a]	0.8
Michaelis–Menten factor for 50% of maximum ion uptake rate [a]	0.4
Upper limit to k_{min} for adequate roots uptake and evapotranspiration [a]	1.0×10^{-5}
N Reallocation coefficient [a]	0.5
NH$_4^+$ in soil root zone (g N m^{-2}) [d]	0.243
NO$_3^-$ in soil root zone (g N m^{-2}) [d]	0.189
Max. NH$_4^+$ nitrification rate (s^{-1}) [a]	2.5×10^{-6}
Max. NO$_3^-$ denitrification rate (s^{-1}) [a]	1.0×10^{-6}
Max. volatilization rate (s^{-1}) [a]	1.0×10^{-9}
N Bio-fixation at reference conditions (g N m^{-2} s^{-1}) [a]	1.0×10^{-7}
N Deposition of (g N m^{-2} yr^{-1}) [e]	0.75
Inorganic fertilization (g N m^{-2} yr^{-1})	0.0
Organic fertilization (g N m^{-2} yr^{-1})	0.0

[a] Arain et al. (2006); [b] Peichl and Arain (2006); [c] Yuan et al. (2008); [d] Peichl and Arain (2007); [e] Environment Canada (2005); [f] Parton et al. (1996).

2.4. Statistical analysis

To analyze the perspective N controls on carbon sequestration and water exchanges, model simulations were performed using both the carbon and nitrogen coupled model (C&N-coupled model) and a carbon-only version of the model (default or non-N model). Apart from comparing simulated and observed carbon (GEP, R_e, NEP) and water (ET) fluxes, modeled soil-plant nitrogen variables were also compared with the field observations, including soil ammonium (NH_4^+) and nitrate (NO_3^-) concentrations, net nitrogen mineralization rate, C:N ratio of soil and leaves and soil surface N_2O fluxes. Linear regression analyses of modelled vs. observed daily carbon and water exchanges were conducted for both N-coupled and default non-N model. Mean absolute error (MAE) and root mean square error (RMSE) were calculated to evaluate the model's performance to explore N controls on carbon and water fluxes.

MAE was determined as:

$$MAE = \frac{1}{N}(\sum_{i=1}^{N}|P_i - O_i|) \tag{10}$$

And RMSE was defined as:

$$RMSE = \sqrt{(\frac{1}{N}\sum_{i=1}^{N}(P_i - O_i)^2)} \tag{11}$$

CHAPTER 3: RESULTS AND DISCUSSION

3.1 Soil-plant nitrogen processes simulation

3.1.1 Diurnal courses of carbon, water and surface conductance

Ensemble diurnal courses of the observed and simulated (N-coupled and non-N model) GEP, ET, and canopy conductance (Gs) values over the growing season (1st Apr to 31st Oct) for five years (2003 to 2007) are shown in Fig. 3. The simulated half-hourly diurnal GEP generally ranged from 0 to a maximum of 17 μmol CO_2 m^{-2} s^{-1}. N-coupled model simulated (solid lines in Fig. 3a) and observed (crosses in Fig.3a) GEP explained 98%, 98%, 92%, 99%, and 95% of the observed variation for 2003-2007, respectively. The N-coupled model was able to capture diurnal GEP physiological changes with a sharp increase in the early morning hours and a gradual decrease after 10:00 a.m. Such diurnal patterns have been observed by other researches as well (e.g. Dai et al., 2004), and is mostly due to nitrogen controls on photosynthetic rates, through Rubisco-N related enzyme controls on carboxylation. The Non-N coupled model overestimated GEP values as compared to observations for all five years (Fig. 3a). A small overestimation of GEP was shown by the N-coupled model during the growing seasons of 2005 and 2007 and slight underestimation during 2003 and 2006 (Fig. 3a). These deviations were caused by climate variations (Fig. 2). There was a spring drought in 2005 and a significant drought throughout the growing season in 2007, which reduced observed GEP values much more as compared to simulated values by the N-coupled model. Meanwhile, 2003 was a mild and wet year and 2006 was the wettest of all five years with warm winter and spring temperatures, which may have contributed to the higher observed GEP values.

Comparison of simulated and measured ensemble canopy conductance values is shown in Fig. 3b. Simulated diurnal Gs curves generally showed the same pattern among years: a sharp increase after sunrise and a maximum in early morning hours followed by a nearly linear decrease until sunset. A similar pattern was observed in other forests (Grelle et al., 1999). Generally, the model simulations showed the same pattern as observed Gs, but with more scatter in observed data during early morning hours. The N-coupled model presented relatively good shape of observations, especially, the so called mid-day depression around 2 pm. Meanwhile yearly variations in Gs were also evident. There is a significant drop in maximum Gs values in 2005, which was probably caused by a spring drought this year. Still, more factors besides N have to be considered to better simulate the stomatal conductance metabolisms at the diurnal scale.

ET simulations showed the same pattern as GEP, with maximum diurnal values of 0.26 mm s^{-1} in 2007 (Fig. 3c). The N-coupled model explained 95%, 96%, 83%, 97%, and 88% of the observed variations in ET for 2003 to 2007, respectively. Meanwhile, the non-N model only explained 88%, 85%, 65%, 95%, and 75% variations for the 5 years, respectively. The improvement in N-coupled model simulated ET was largely due to N controls on photosynthesis and stomatal conductance.

Nitrogen controls, in our model, were largely due to the Rubisco-N related enzyme controls on photosynthesis, which is basically expressed as the limitation of leaf N content on carboxylation. On the diurnal time scale, N related control occurs when temperature increases around noon, and when light or transport capacity is not a limitation.
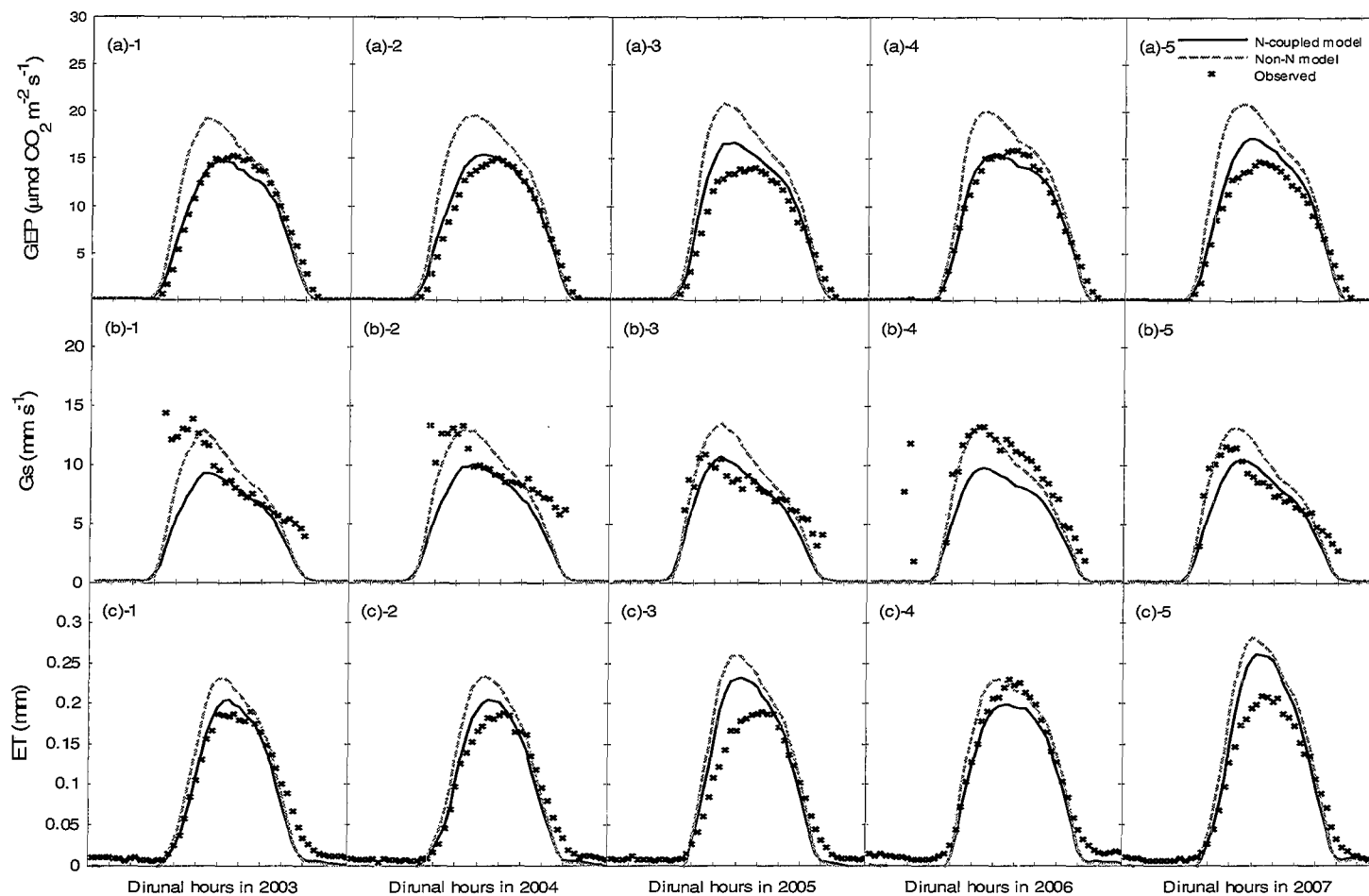
Figure 3: Comparison of observed and simulated (N-coupled model and non-N model) growing seasonal (Apr. – Oct.) ensemble diurnal values of (a) gross ecosystem productivity (GEP), (b) canopy conductance (Gs), and (c) evapotranspiration (ET) for five years (2003 to 2007) at TP39.

3.1.2 Soil nitrogen dynamics

Simulated soil-plant nitrogen processes (e.g. soil N mineralization, nitrification, denitrification, NH_4^+ and NO_3^- concentrations, soil surface N_2O fluxes, C:N ratios, as well as plant root N uptake and leaf Rubisco-N content) are presented along with observed field measurements in Table 3 and Figure 4 and 5.

Simulated soil N_2O production rates showed a diverse pattern over an annual course as shown in Fig. 4. Generally, the simulated N_2O flux was higher during the summer months and lower during winter. Hourly N_2O fluxes were measured at this site in 2007 using a closed-chamber system as described in Peichl et al. (2009a). Simulated N_2O values showed reasonably good agreement with temporal dynamics and magnitude of observations. An N_2O emission spike was simulated in the early of August, and also showed a sharp decrease during the same month. These extremes may have been caused by extremely dry weather conditions in the summer followed by large precipitation events in late summer or early autumn causing large variations in soil water and temperature in the sandy soils of this forest site. Some underestimation occurred in April (during the spring defrosting period) and December (during the winter freeze time). The production of N_2O in soils is a complicatedly process that is influenced by soil temperature, soil moisture, oxygen availability, nitrogen status of substrate (NH_4^+ and NO_3^-), and soil carbon availability (Billings, 2008; Calanca et al., 2007; Firestone and Davidson, 1989; Frolking et al., 1998; Goldberg and Gebauer, 2008; Li et al., 2000). More field observations and laboratory experiments are still needed to fully understand N_2O production and emission processes.

The simulated N mineralization rates ranged from a minimum of 9.4 mg N m^{-2} day^{-1} during the winter seasons in 2003 to a peak value of 53.2 mg N m^{-2} day^{-1}

during the early August in 2006 (data not showed). In general, mean N mineralization rates showed higher values in the summer (May to September) and lower values in winter and early spring. In 2005 and 2006, simulated N mineralization rates (8103 and 7600, mg N m^{-2} year^{-1}, respectively) were generally higher than in other study years. 2005 had the highest annual air temperature during the growing season with near normal annual precipitation despite a spring drought, while 2006 had near-record warm temperatures and the highest cumulative daily precipitation values (Fig. 2). Simulated N mineralization rates were low (7211 and 7364 mg N m^{-2} year^{-1}, respectively) during years with colder and drier climatic conditions. A large spike in the N mineralization rate on August 2nd (day of year, DOY 214) in 2006 was closely correlated with the large precipitation and high air temperature (data were not shown). The observed dry and cold winter of 2003 had the lowest value of N mineralization rate (~9 mg N m^{-2} day^{-1}) of five years. Similar trends in N mineralization rates have been observed in field-based studies in the literature (Bonito et al., 2003; Ullah and Moore, 2009; Zak and Grigal, 1991). Ullah and Moore (2009) showed a comparison of N transformation rates among well- and poorly-drained forest sites in Southern Quebec, Canada. Their average observed N mineralization rates ranged from 38 ± 6 mg N m^{-2} day^{-1} in well-drained soils to 17 ± 5 mg N m^{-2} day^{-1} in poorly-drained soils. And their reported seasonal trends of well-drained soil were comparable with simulated rates at our site in Southern Ontario with the similar drainage characteristics (Table 3).

Overall, simulated seasonal and five-year mean values of nitrification rates were in good agreement with field observations at our site, and showed a clear tendency of higher nitrification rates from June to September (Table 3). There appeared to be no clear inter-annual variability in nitrification rates, with daily

values ranging from 0.2 mg N m^{-2} day^{-1} during the winter to 11.2 mg N m^{-2} day^{-1} in the summer.

Modeled denitrification, however, showed a different seasonal trend and relatively smaller inter-annual variability as compared to N mineralization and nitrifications trends. Generally, denitrification rates were higher in late winter and spring and lower in summer and autumn. The five-year mean value was comparable with field studies in forests (e.g. Wolf and Brumme, 2003) (Table. 3).

Simulated soil NO_3^- and NH_4^+ concentrations, considered as the primary soil-plant nitrogen cycle connections between plant N uptake and soil N supply, were also strongly correlated with the seasonal dynamics of observed environmental variables such as temperature and precipitation. Highest values of NO_3^--N and NH_4^+-N were observed in summer months, when soil temperature reached its maximum. Inorganic nitrogen ion concentrations in soil are directly related to organic soil mineralization and plant nitrogen uptake rates, because of contribution from other nitrogen input sources (e.g. bio-fixation and atmospheric deposition). Simulated NO_3^- and NH_4^+ concentration values were qualitatively consistent with the observations made using the buried-bag incubation method at this site during the 2006 and 2007 growing seasons (Peichl et al., 2009a) (Table. 3).

Similarly, simulated C:N ratios for the top 10 cm of the soil column was 19.5 as compared to observed value of 15.4 (Table. 3).
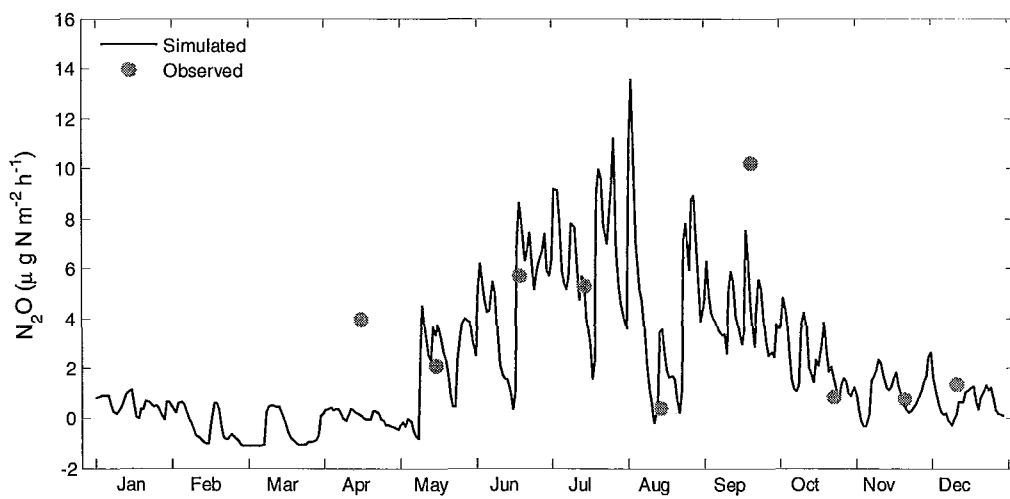
Figure 4: Comparison of simulated half-hourly soil surface nitrous oxide (N_2O) fluxes with measured values in 2007.

Table 3: Comparison of simulated and observed net nitrogen mineralization, nitrification and denitrification rates, soil ammonium (NH_4^+) and nitrate (NO_3^-) concentrations, C:N ratio in 0-10 cm soil column and C:N ratio in leaves for Turkey Point mature forest site.

	Period	Observed	Modeled
N mineralization $(mg\ N\ m^{-2}\ day^{-1})$	Apr.	-3 ± 3.6 [b]	12.4
	Jun.-Aug.	42 ± 1.5 [b]	39.3
	Sept.-Nov.	20 ± 1.5 [b]	26.5
	Annual mean	12~44 [b]	24.0*
Nitrification $(mg\ N\ m^{-2}\ day^{-1})$	Apr.	3 ± 5.9 [b]	1.1
	Jun.-Aug.	16 ± 15.9 [b]	8.8
	Sep.-Nov.	9.3 ± 11.3 [b]	9.9
	Annual mean	3~22 [b]	10.4*
Denitrification $(mg\ N\ m^{-2}\ day^{-1})$	Annual mean	0.144 [c]	0.9*
NH_4^+ $(mg\ N\ m^{-2})$	2006: Aug. 2-28	418.5 ± 40.5 [a]	589.6
	2007: Jul. 16-Aug.10	108 ± 121.5 [a]	224.4
	2007: Oct.24-Nov. 21	216 ± 13.5 [a]	357.8
	Annual mean	683 ± 59 [b]	721.4*
NO_3^- $(mg\ N\ m^{-2})$	2006: Aug. 2-28	148.5 ± 13.5 [a]	143.0
	2007: Jul. 16–Aug.10	189 ± 27 [a]	160.3
	2007: Oct. 24–Nov.21	229.5 ± 13.5 [a]	292.4
C:N ratio in soil (0-10cm)	Annual (2006)	15.4 [a]	19.5
C:N ratio in leaf	Annual (2005)	38.165 [d]	33.4

[a] Peichl et al., 2009a; [b] Ullah and Moore, 2009; [c] Wolf and Brumme, 2003; [d] Flanagan, 2005; * Annual mean value of 2003 to 2007.

3.1.3 Plant nitrogen dynamics

Simulated daily plant nitrogen uptake rates, and leaf Rubisco-N content (Rubisco-N) in the top canopy are presented in Fig. 5. Both plant N uptake and leaf Rubisco-N content showed strong seasonal and inter-annual variability.

Simulated mean daily plant N uptake rates experienced diverse courses during the growing season (Fig.5a~e), ranging from 98 mg N m^{-2} day^{-1} in the peak growing season to near zero in winter (Fig. 5a~e). A large increase occurred in April (DOY 90-120), followed by a decline during May to June (DOY 140-150), after which uptake rate remained relatively constant until late autumn, sharply declining during the winter season. This pattern of variation was possibly a result of fast leaf development and expansion during the early spring, with a larger demand for nitrogen uptake, which is indicated as the large rise in plant N uptake in the early growing season. Small changes during the summer indicate a relatively stable plant nitrogen demand following leaf formulation. During the late growing season, plant nitrogen uptake rate decreased as leaf senescence started in the autumn. Similarly, a leaf nitrogen content decrease during early spring has also been observed by other researchers (Grassi et al., 2005). Grassi et al., has found that leaf nitrogen started to recover in mid-summer (July) due to continuous nitrogen uptake by the forest.

Rather than a fixed value in the default non-N model, the maximum carboxylation capacity (V_{cmax}) in CLASS-CTEM^{N+} is controlled by the leaf nitrogen content, and thus, is determined by the coupling of soil and plant C and N cycles. Compared to the plant root N-uptake, the seasonal variability of leaf Rubisco-N content ranged from 0.46 g N m^{-2} LAI^{-1} in early spring, when leaves

were developing, to 0.57 g N m^{-2} LAI^{-1} in the peak growing season when forest LAI was at its maximum. This value declined in autumn, when leaves started to senescence (Fig. 5f). Comparing years, 2004 and 2007 had lower leaf Rubisco-N content values during the spring, while 2003 showed lower values in autumn and winter. This might also be explained by the yearly variation of climate conditions, where a warm and wet climate induced higher leaf N content. Despite these annual dynamics, the relatively small value for leaf Rubisco-N content indicates a very small inter-annual variability in this temperate conifer forest.

Simulated annual mean leaf C:N ratio of 33.4 was in good agreement with the value of 38.2 observed during the 2005 field campaign (Table 3). Modeled stem and root C:N ratios, showed similar but more stable variations compared to leaf C:N ratio changes (data not shown).
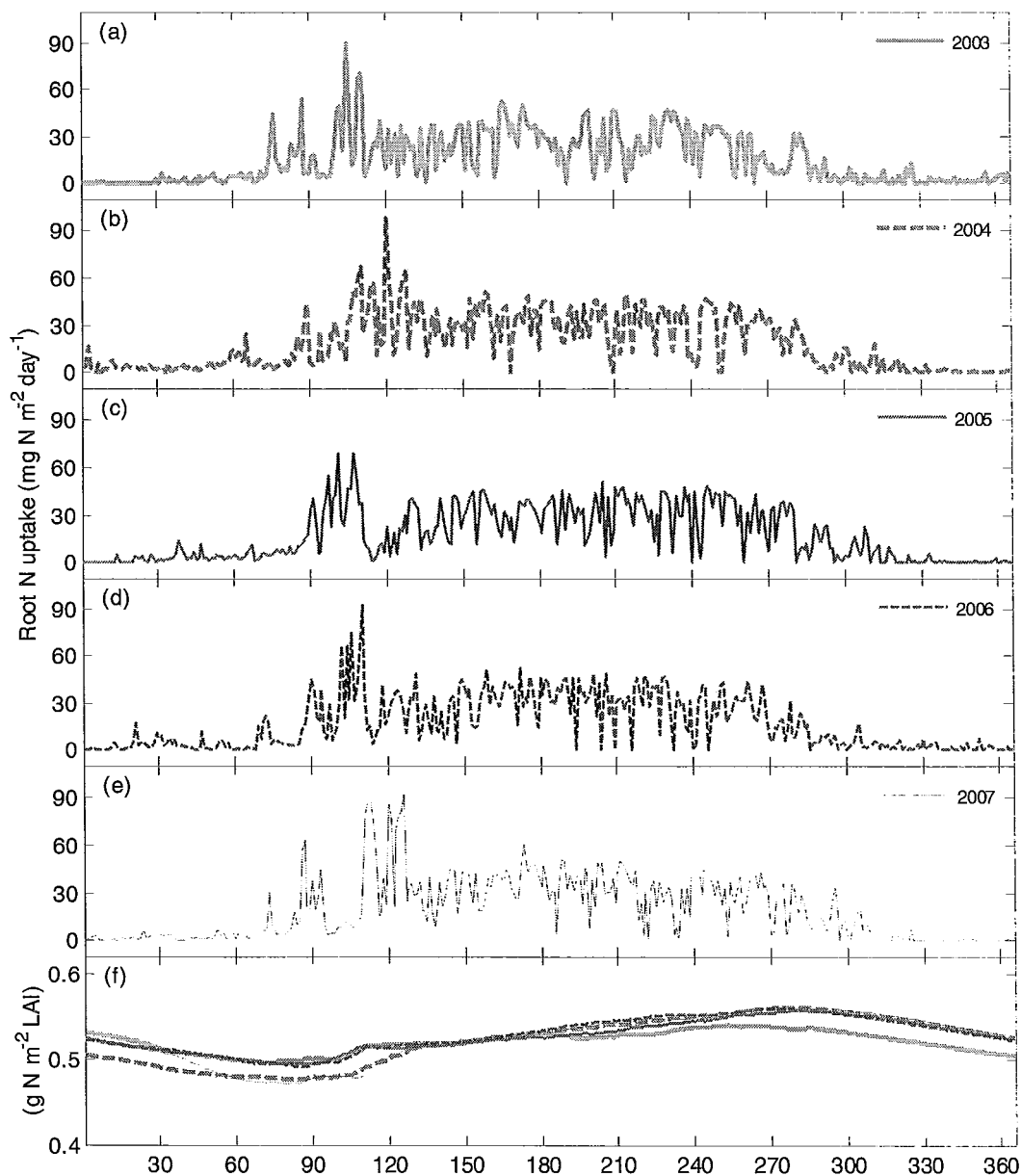
Figure 5: Simulated daily (a~e) plant N uptake rate (mg N m^{-2} day^{-1}); and (f) leaf Rubisco-N content at top canopy (g N m^{-2} LAI^{-1}) from 2003 to 2007.

3.2 Nitrogen controls on carbon and water exchanges

3.2.1 Impact of N controls on daily carbon and water fluxes

Simulated daily carbon and water fluxes using N-coupled and non-N coupled models were compared with observed eddy covariance (EC) fluxes over the study period (2003-2007) (Fig. 6). GEP, R_e, NEP, and ET values were in better agreement with observations for the N-coupled scheme (with RMSE of 1.97, 0.73, 1.44, 0.92; and MAE of 1.48, 0.55, 1.01, 0.60; n=1825 for GEP, R_e, NEP, and ET, respectively) as compared to the non-N model (with respective RMSE of 2.95, 1.35, 1.93, 1.03; MAE of 2.38, 1.15, 1.55, 0.71; n=1825). These results clearly indicated improvements in carbon and water simulation capabilities due to the incorporation of N constraints in the model. The non-N model showed an overestimation of GEP, largely because the photosynthesis controlling parameter V_{cmax} is prescribed in the default model rather than by a dynamic estimation through soil-plant nitrogen processes in the N-coupled model. While R_e is indirectly related to soil-plant N status through assimilation and soil carbon cycling, R_e would not respond to the nitrogen cycle as quickly as GEP. Fig. 6c-d showed a slight overestimation of R_e in non-N simulations compared to N-coupled results. Thus, different magnitudes of nitrogen controls on both GEP and R_e are reflected in simulated NEP (Fig. 6e, f). The correlation between measured and simulated ET values (Fig. 6g, h) showed that the N-coupled model simulations provided slightly better correlation than the non-N model. This indicates that the introduction of soil-plaint nitrogen cycling has enhanced the simulation of ET, but to a lesser extent than with N controls on carbon sequestration.
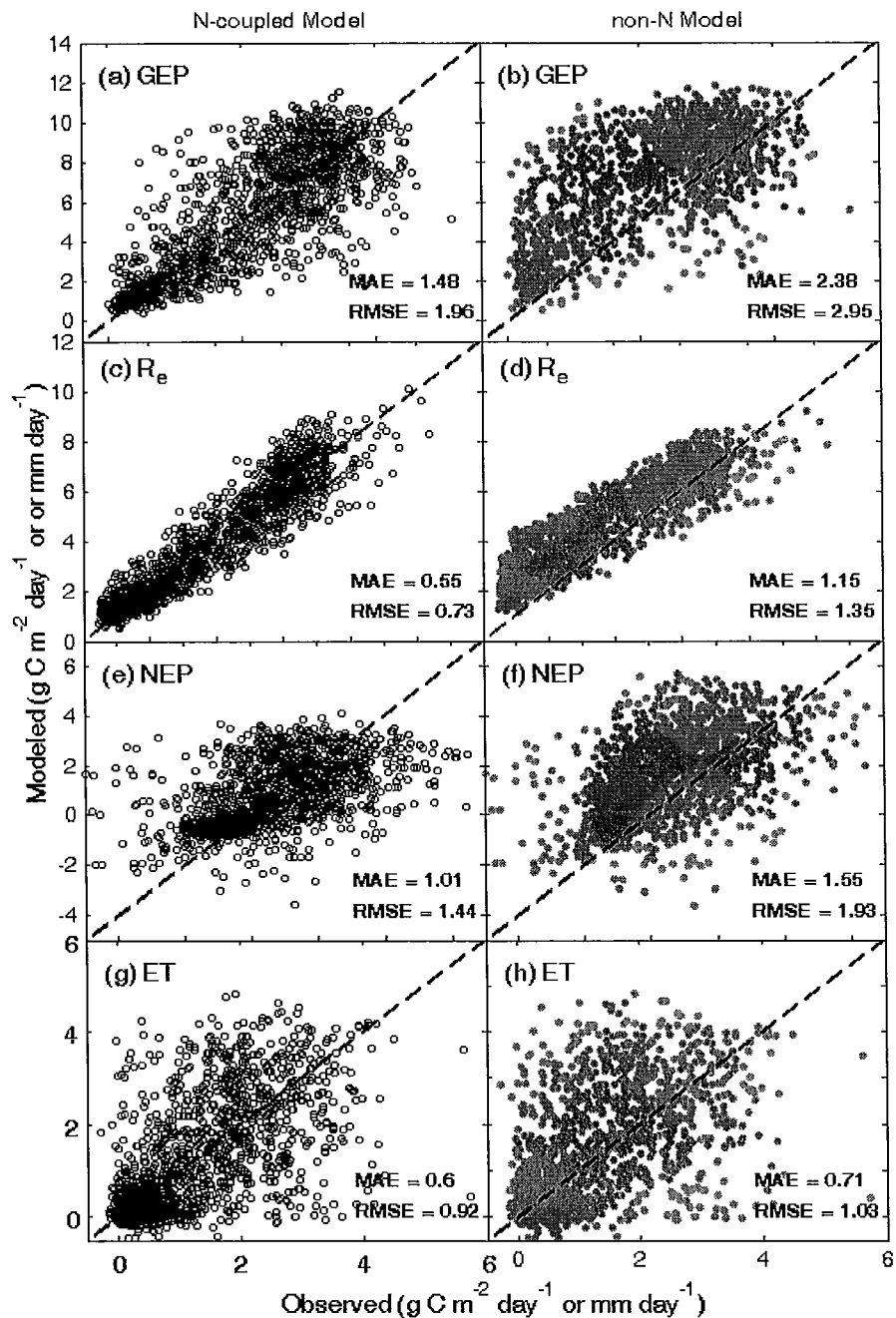
Figure 6: Comparison of observed daily gross ecosystem productivity (GEP), ecosystem respiration (R_e), net ecosystem productivity (NEP), and daily evapotranspiration (ET) values with simulated values by the N-coupled model (a, c, e, g) and non-N model (b, d, f, h), respectively, from 2003 to 2007.

3.2.2 N controls on seasonal carbon and water variations

Time series of observed and simulated daily carbon fluxes by N-coupled and non-N coupled models are shown in Figure 7. Both models effectively captured the intra-annual (seasonal) variability in GEP, R_e and NEP, with high values in the summer and low values in winter. Seasonal dynamics of nitrogen controls were clearly observed because N-coupled simulated values were in better agreement with observation (Fig. 7a-c). Seasonal variations in GEP were overestimated by the non-N model, especially during the winter and early spring seasons (Fig. 7a). This is largely due to the fixed value of V_{cmax} used in the default model as compared to nitrogen controls on the photosynthesis enzyme activities in the N-coupled model as discussed previously. During the peak growing season, no obvious differences were present between the two models. The non-N model simulated peak daily GEP values are 12.5 (13-June), 12.2 (15-June), 11.7 (16-June), 11.3 (08-June) and 12.4 (13-June) g C m^{-2} day^{-1}, compared to 11.9 (13-August), 12.45 (15-June), 12.4 (18-July), 12.6 (12-July) and 12.1 (13-August) g C m^{-2} day^{-1} by the N-coupled model; and 11.6 (11-July), 11.1 (30-June), 10.8 (16-June), 11.1 (27-June) and 12.9 (04-June), g C m^{-2} day^{-1} from observations over the five years, respectively. In the warm and wet years of 2005 and 2006, the discrepancy between simulated and observed fluxes was mainly due to higher photosynthetic uptake sensitivity to temperature (Arain et al., 2009). In cooler years (e.g. 2003), this underestimation was not present. Overall, the incorporation of nitrogen controls on photosynthetic uptake through V_{cmax} has clearly showed improvements in simulated GEP values on seasonal scales.

The same pattern was observed for R_e (Fig. 7b). Both models performed very well in simulating R_e and there was much less spread between observed and

simulated daily values. The maximum simulated R_e values were 7.7 (14-August), 7.8 (01-August), 8.7 (18-July), 9.0 (01-August) and 8.0 (14-August) g C m^{-2} day^{-1} for non-N simulations; and peaked 8.4 (13-August), 8.2 (21-July), 9.3 (18-July), 10.0 (1-August) and 8.2 (13-August) g C m^{-2} day^{-1} for N-coupled model, as compared to maximum observed values of 8.1 (15-August), 7.4 (23-July), 7.7 (25-September), 10.4 (31-July), 7.6 (12-August) (g C m^{-2} day^{-1}) over the five years, respectively. These results indicate that the respiratory CO_2 fluxes in this mature temperate conifer forest are more sensitive to variations in temperature as compared to nitrogen controls, unless they are through GEP effects in autotrophic respiration.

Significant improvements in the simulated seasonal dynamic of NEP were demonstrated by the N-coupled model, while NEP simulated by the non-N scheme was much higher compared to observations, especially during the spring months (Fig 7c). Similarly, in winter (mostly from December to February), the non-N scheme simulation overestimated carbon sequestration. Generally, there were two simulated NEP peaks, one in May-June and one in September, indicating high carbon uptake during these periods. These peaks result from low temperature and humidity in the early spring season (Fig. 2), leading to higher GEP compared to R_e. In contrast, during the summer months, respiration increased more than photosynthesis, resulting in a mid-summer decline in NEP. Daily net primary productivity (NPP) reached its highest value of 6.7 g C m^{-2} day^{-1} around May, when LAI was the highest and climate conditions were favorable for maximum CO_2 uptake. Both versions of the model simulated these phenomena very well. Some of the scatter between observed and simulated NEP values may be due to the uncertainty in observations, since eddy covariance system performs poorly during low turbulent conditions and there might be other system errors as well. These results further showed that spring and early summer was a crucial

period to determine annual carbon uptake in this forest and variations in NEP from May to August would largely determine the difference in inter-annual NEP values. Overall, nitrogen controls had a much greater effect on GEP and NEP than R_e on an intra-annual basis.

Figure 8 shows the seasonal dynamics of daily ET values simulated by both models when compared with observations. Both N-coupled and non-N simulations were able to capture daily and intra-annually variations in the measured evaporative fluxes. The N-coupled model simulated ET values were in good agreement with observations from June through September, while the non-N model either over- and under-estimated ET during these periods. The underestimation of ET in July and August of 2003 and 2004 and its overestimation in September 2005 was largely due to warmer summer temperatures. Improvement in ET values from N-coupled model was mostly a results of the incorporation of leaf Rubisco-N modulated photosynthesis algorithms in the N-coupled model, which exerted interactive control on canopy conductance and transpiration (Dickinson et al., 2002). Thus, the improved carbon assimilation also resulted in improved in partitioning of energy and water fluxes.

On the seasonal scale, nitrogen controls were more pronounced during the non-growing season. This was mostly due to the N-related V_{cmax}, incorporated in the N-coupled model as compared to the fixed prescribed value in the non-N model. The incorporation of leaf Rubisco-N modulated photosynthesis algorithms in the N-coupled model, which interact with other soil-plant N cycling processes as well, have also improved the seasonal dynamics of evapotranspiration simulations, particularly during the main growing season.
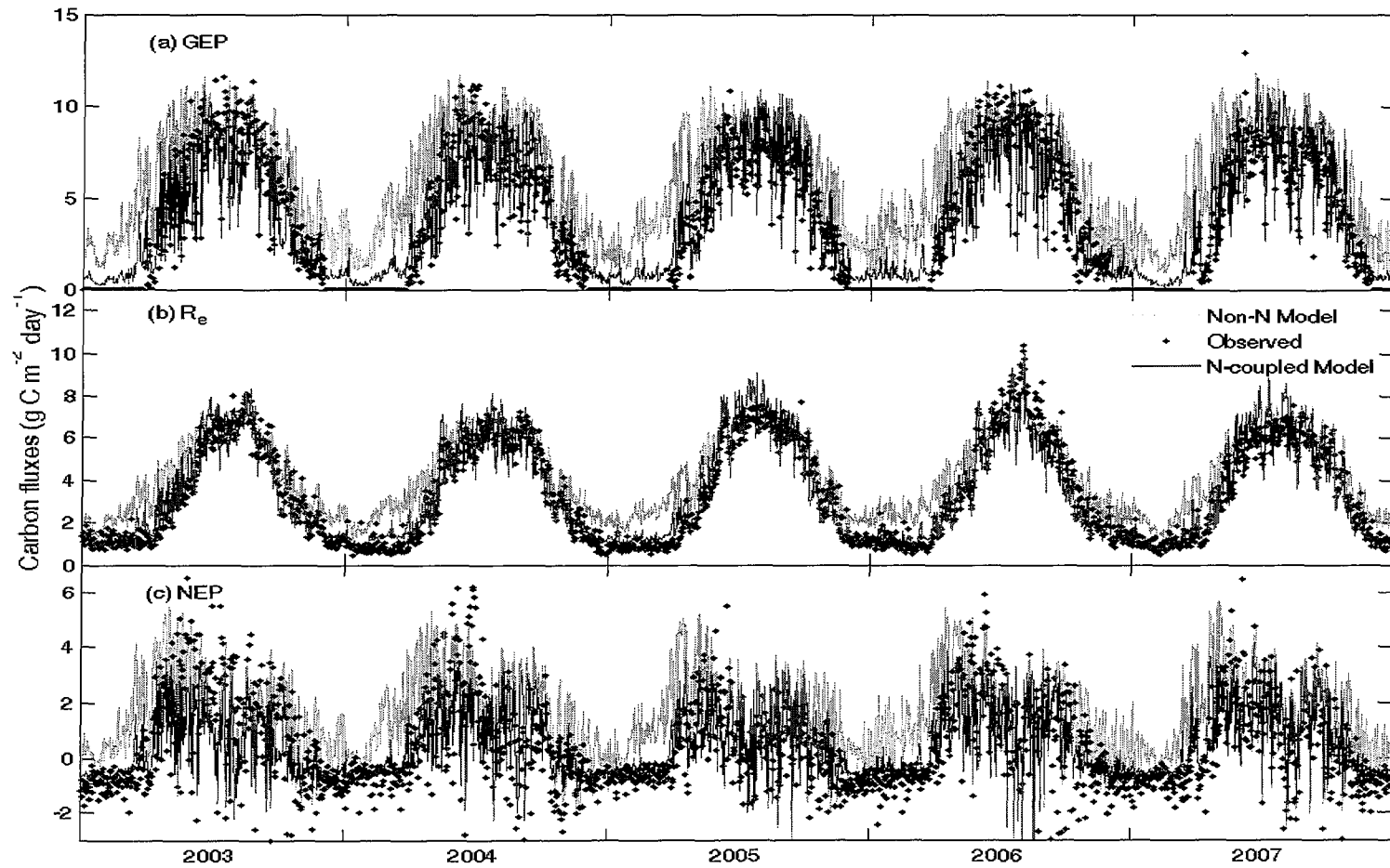
Figure 7: Daily gross ecosystem productivity (GEP), ecosystem respiration (R_e) and net ecosystem productivity (NEP) values simulated by the N-coupled model (black line) and non-N model (grey line) compared with measurements (black dots) from 2003 to 2007.
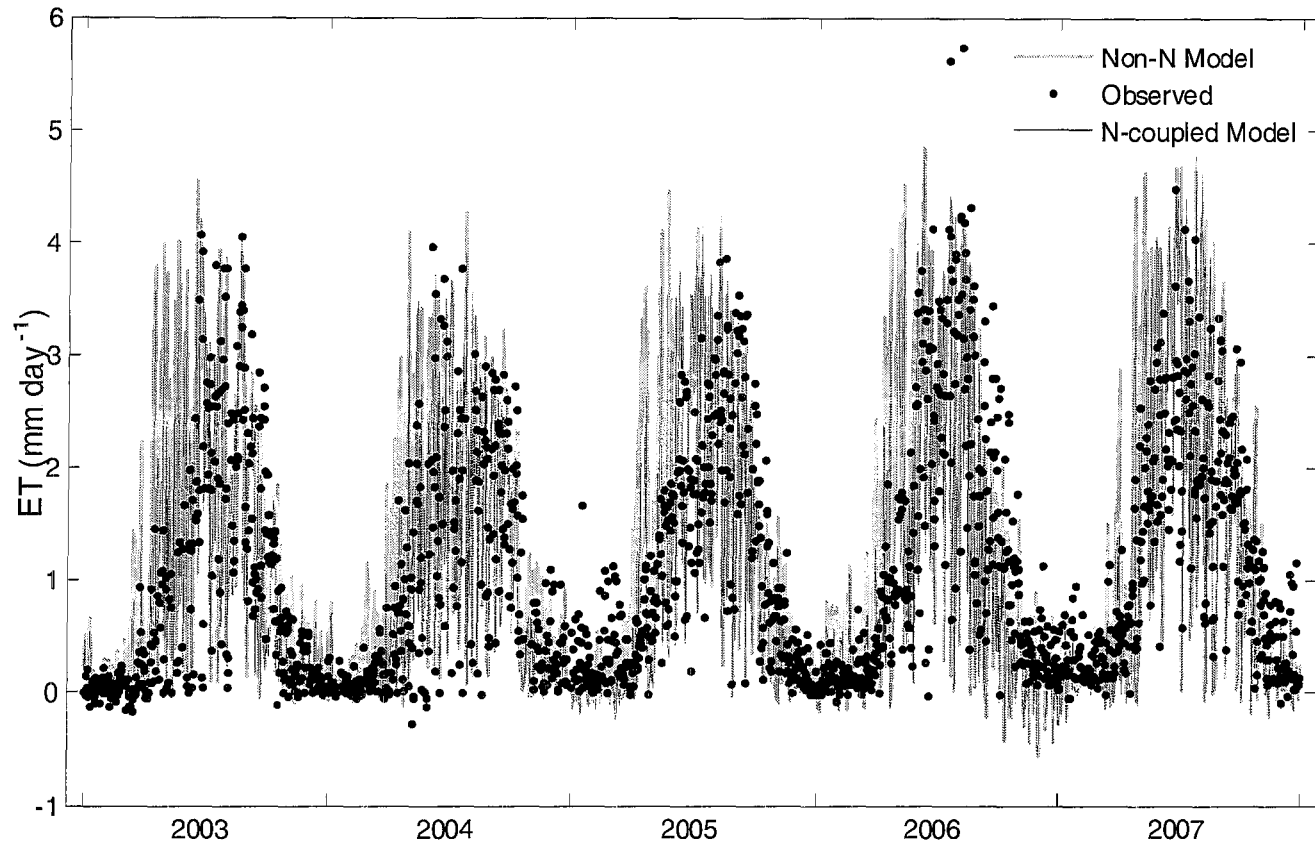
Figure 8: Daily evapotranspiration (ET) values simulated by the N-coupled model (black line) and non-N model (grey line) compared with measurements (black dots) from 2003 to 2007.

3.2.3 N controls on inter-annual variability

Measured and simulated annual GEP, R_e, NEP and ET values for 2003-2007 are given in Table 4. The N-coupled model simulated annual GEP values over the five years were 1425, 1489, 1578, 1536 and 1589 g C m^{-2} yr^{-1}, with 5-year mean value of 1524 g C m^{-2} yr^{-1}. Observed GEP values were 1387, 1309, 1278, 1458 and 1337 g C m^{-2} yr^{-1} for five years, respectively, with 5-year mean value was 1354 g C m^{-2} yr^{-1}. Non-N-coupled model simulated annual GEP values were 2122, 2183, 2210, 2200 and 2209 g C m^{-2} yr^{-1}, with 5-year mean value of 2185 g C m^{-2} yr^{-1} (Table. 4). The N-coupled model was in better agreement with observations. The related standard deviations (S.D.) were 68, 37 and 71 g C m^{-2} yr^{-1} for the N-coupled, Non-N simulations and observations, respectively, indicating relatively small inter-annual variability among both measured and simulated values.

The model performed very well for annual R_e simulations, with 5-year mean values of 1231, 1278 and 1590 g C m^{-2} yr^{-1}, for observed and N-coupled and non-N coupled model results, respectively; and with S.D of 57, 42 and 45 g C m^{-2} yr^{-1}, respectively.

There was a slight overestimation of simulated annual NEP values by the N-coupled model (Table. 4), largely due to the overestimated GEP (Table 4). 2005 has lowest observed NEP of 33 g C m^{-2} yr^{-1}, which was due to the spring drought and near record summer warming in that year. Meanwhile, the model was unable to simulate the impact of these extreme events on the annual carbon budget.

Observed annual ET values were 296, 280, 382, 439 and 426, with a 5-year mean value of 365 and S.D. of 73 mm yr^{-1}. The N-coupled model simulated

annual ET values of 347, 346, 383, 384 and 442 (5-year mean value of 380 with S.D. of 39, mm yr^{-1}). They showed a clear improvement as compared to the non-N model (420, 420, 452, 470 and 507 mm yr^{-1}, with 5-year mean value of 454 and S.D. of 37, mm yr^{-1}).

Table 4: Comparison of observed annual gross ecosystem productivity (GEP), ecosystem respiration (R_e) and net ecosystem productivity (NEP) in g C m^{-2} yr^{-1} and evapotranspiration (ET) in mm yr^{-1} with simulated values by the N-coupled model and default non-N model from 2003 to 2007.

		2003	2004	2005	2006	2007	5-year mean	S.D.
GEP	N-coupled	1425	1489	1578	1536	1589	1524	68
	Non-N	2122	2183	2210	2200	2209	2185	37
	Observed	1387	1309	1278	1458	1337	1354	71
R_e	N-coupled	1244	1247	1346	1264	1287	1278	42
	Non-N	1529	1564	1643	1601	1614	1590	45
	Observed	1175	1191	1239	1322	1229	1231	57
NEP	N-coupled	134	195	183	225	255	199	46
	Non-N	535	562	507	540	535	536	20
	Observed	220	126	33	142	102	125	67
ET	N-coupled	347	346	383	384	442	380	39
	Non-N	420	420	452	470	507	454	37
	Observed	296	280	382	439	426	365	73

3.3 Sensitivity analysis

3.3.1 Sensitivity analysis of climate controls

An analysis was conducted to evaluate Models' sensitivity to simulate carbon and water fluxes under varying environmental conditions and nitrogen cycle feedbacks. Selected forcing variables that are most relevant to global climate change were increased and decreased for this analysis (for detailed methods used, refer to section 2.3 at page 13-14). Results showed that the model is most sensitive to changes in atmospheric CO_2 concentration and air temperature (Fig. 9, left panel). An increase in CO_2 concentrations caused the maximum increase in GEP, which increased from 1375 to 1685 g C m^{-2} year^{-1} (Fig. 9a). Similarly, CO_2 variations induced the largest increases in R_e (Fig. 9c); and NEP (Fig. 9e). However, CO_2 changes only introduced minor variations in ET values (Fig. 9g).

Air temperate demonstrated a strong influence on ET, with an 87% decrease occurring for a 1.0 °C decrease in Ta. An increase of 18% was observed for 1.0 °C warming. Generally, Ta had a positive impact both on GEP and R_e, with -3%, -2%, +2% and +3% change for the prescribed Ta changes ranging from ± 0.5 °C and ± 1 °C. However, Ta sensitivity tests showed a very clear negative trend for NEP. Generally, increase in Ta promoted higher R_e, while only slightly enhancing GEP. Overall, the contrasting responses of carbon uptake and release to site-specific temperature variations resulted in slight decreases in annual NEP with increasing Ta (Fig. 9).

Annual GEP, R_e, NEP and ET showed no significant responses to variations in precipitation (Fig. 9, left panel). This may indicate that in our model, forest growth is not constrained by water availability. While simulated GPP, R_e, NEP

and ET all showed small positive responses to variations in solar radiation (Fig. 9, left panel). Changes in solar radiation caused more variations in NEP than other carbon fluxes with -7%, -3%, 3% and 5% change in NEP, compared to -2%, -1%, 1%, 2% change in GEP, -1%, -1%, 1%, 1% change in R_e, and -4%, -2%, 2%, 4% change in ET, corresponding to the four testing levels of solar radiation, respectively. Higher solar radiation affected GEP directly, and R_e indirectly through higher autotrophic (growth) respiration, as well as heterotrophic respiration due to increased in litter/soil temperatures. As a result, NEP was also affected.

3.3.2 Sensitivity analysis of nitrogen controls

Nitrogen deposition changes showed the largest variations in carbon and water fluxes when compared with N fertilization applications or N:C ratio increases (Fig. 9 right panel). As the nitrogen deposition input was increased incrementally from 0 to 2.75 g N m^{-2} yr^{-1}, the corresponding GEP values were 1585, 1597, 1600 (benchmark value), 1602 and 1607 (g C m^{-2} $year^{-1}$). Similarly R_e values were 1251, 1257, 1259 (benchmark), 1260 and 1262 g C m^{-2} $year^{-1}$; NEP values were 287, 294, 295 (benchmark), 296 and 298 g C m^{-2} $year^{-1}$; and ET values were 258, 260, 260 (benchmark), 261 and 262 mm $year^{-1}$, for the five tested scenarios, respectively. Therefore, the maximum increase in carbon sequestration due to nitrogen deposition was 25 g C per g N for GEP, 12 for R_e and NEP. Our results are much lower than Reay et al. (2008) who reported an increase in carbon uptake ranging from 40 to 200 g C per g N. Janssens and Luyssaert (2009) argued that the carbon uptake per unit nitrogen deposition could vary between zero and several hundred grams of carbon, depending on the spatial variations in site fertility and the differences in the vegetation mechanisms by which nitrogen affects carbon storage. Initial soil N measurements indicates that our forest site is nitrogen limited with well drained sandy soils (Peichl et al., 2009a); therefore an increase in N deposition may not be expected to have much impact on the carbon sequestration.

Simulated carbon and water fluxes showed similar positive responses to nitrogen fertilization application. GEP, R_e, NEP and ET values increased by 4, 2, 2 and 0.7% as fertilization was increased from 0 to 1 g N m^{-2} yr^{-1}. When fertilization was increased from 2, 3 to 5 g N m^{-2} yr^{-1}, simulated GEP increase rates were subdued. This is probably due to the nitrogen saturation effect, as

reported by researchers such as Magnani et al., (2007) in a boreal forest. Still, more detailed aspects needs to be evaluated to obtain a complete understanding of nitrogen cycle feedbacks. Excess N input and N source changes may impact soil acidification, ground and surface water quality, biodiversity, and ecosystem services (De Schrijver et al., 2008).

The sensitivity of C:N ratio changes in litter did not show a significant impact on carbon and water feedbacks, as compared with nitrogen deposition and fertilization changes. There were both positive and negative responses in GEP while positive responses were seen in R_e, NEP and ET. A change of -1.66, -0.31, 0.23 and 1.05 g C m^{-2} year^{-1} was observed in GEP when initial litter C:N ratio was increased by ± 10% and ± 20% with benchmark value of 0.048 (Fig. 9-right panel). Similar minor trends were also observed for R_e, NEP and ET.

Overall, the sensitivity analysis has indicated that variations of solar radiation, air temperature, precipitation and atmospheric CO_2 concentrations would have major impact on carbon sequestration in this forest ecosystem with CO_2 concentration and air temperature being the major controls. Nitrogen deposition/fertilization inputs and litter C:N ratios showed relatively minor feedbacks on carbon sequestration and water exchanges in this study. Nitrogen saturation effect was observed under increased application of fertilization. This analysis demonstrates that land surface schemes must take into account nutrient cycling related feedbacks. The C and N coupled model has the capability of analyzing nitrogen controls and feedbacks on ecosystem under future climate changes. However, further studies are needed for more detailed understanding of the nitrogen cycle processes and feedbacks on ecosystem functions.

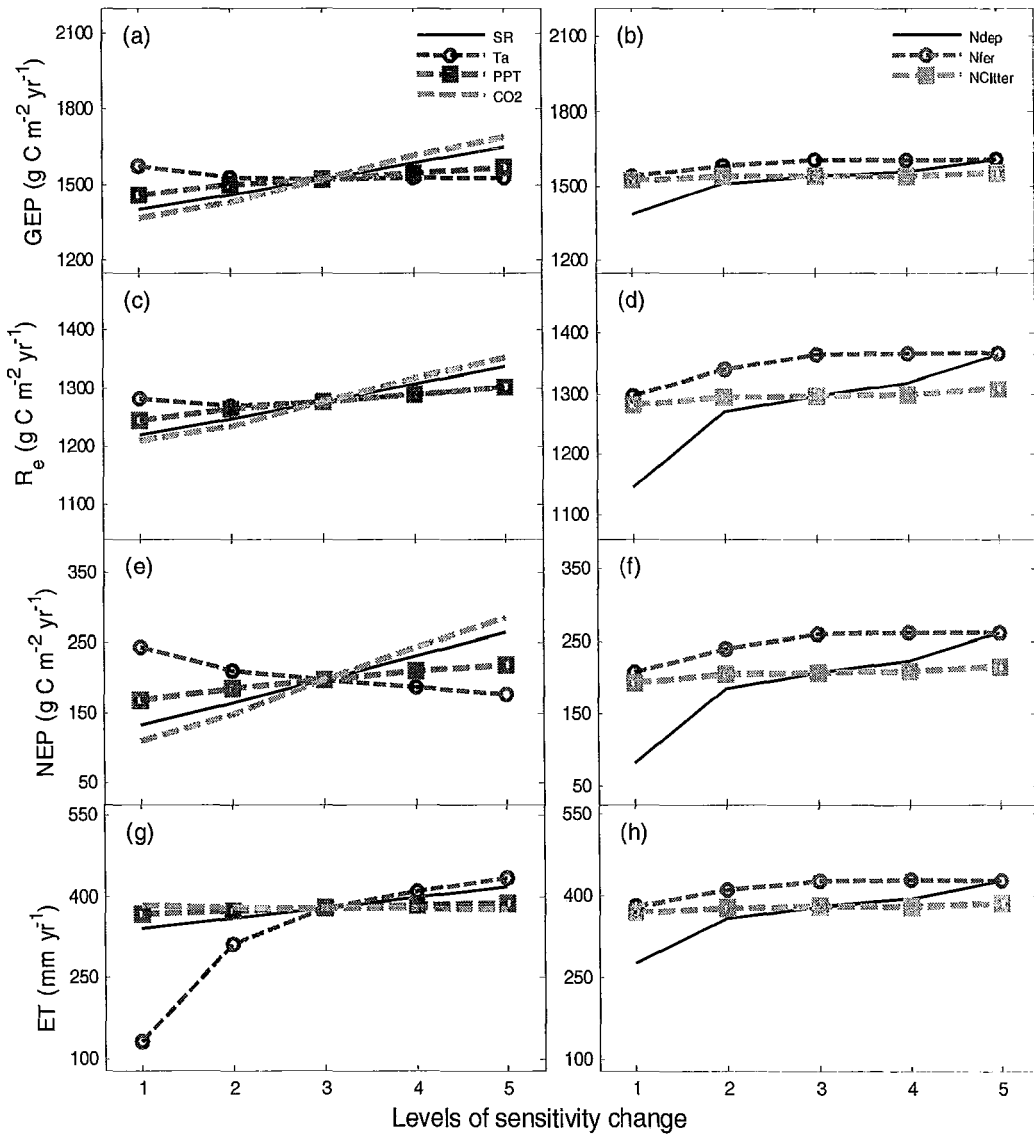**Figure 9:** Sensitivity of annual GEP, R_e, NEP and ET to climate variations including incident solar radiation (SR), air temperature (Ta), precipitation (PPT) and atmospheric CO_2 concentration (CO_2) (panels, a, c, e, g on left had side) and changes in nitrogen variables including N deposition (Ndep), N fertilization (Nfer) and initial N:C ratio in litter (NClitter) (panels b, d, f, h on right hand side).

CHAPTER 4: CONCLUSION

A carbon and nitrogen coupled model--CLASS-CTEM^{N+} was developed by incorporating key soil and plant N cycling algorithms. By comparing simulated N-coupled and non-N coupled) and observed carbon, water and nitrogen exchanges in a 70-year old temperate conifer forest from 2003 to 2007, nitrogen has been identified as an important controlling factor in this ecosystem and responses and feedbacks cannot be ignored.

Simulated plant nitrogen variable such as V_{cmax} and plant N uptake rate showed clear seasonal and annual variations, and were compared reasonably well with the field observations during the study period. Comparison of N-coupled model simulated gross ecosystem productivity (GEP), ecosystem respiration (R_e) and net ecosystem productivity (NEP) with measured eddy covariance fluxes over 5 years showed a better agreement (RMSE of 1.96, 0.735, 1.44 with MAE of 1.48, 0.55, 1.01 for GEP, R_e and NEP, respectively; n=1825) as compared to default non-N model (RMSE of 2.95, 1.35, 1.93 with MAE of 2.38, 1.15, 1.55 for GEP, R_e and NEP, respectively; n=1825). Impact of N limitation was also observed in simulated evapotranspiration (ET) exchanges (RMSE of 0.92 and MAE of 0.60 for N-coupled model as compared to RMSE of 1.03 and MAE of 0.71, n=1825, for default non-N model when compared with measured ET values). Sensitivity analysis conducted for key environmental factors (such as solar radiation, air temperature, precipitation and atmospheric CO_2 concentrations), showed that changes in CO_2 concentrations had major impact on forest carbon exchanges, while air temperature was a major control on evapotranspiration. Changes in nitrogen deposition/fertilization inputs and litter C:N ratio affected carbon

44

sequestration and water exchanges, with increasing nitrogen saturation effects under increased application of fertilizers.

In our model, nitrogen impacts were largely due to the Rubisco-N related enzyme controls on photosynthesis, which is expressed as the limitation of leaf N content on carboxylation. On the diurnal time scale, N related control occurred when temperature increases around noon, and when light or transport capacity was not a limitation. On the seasonal scale, nitrogen controls were more pronounced during the non-growing season. This was mostly due to the N-related $V_{cmax,}$ incorporated in the N-coupled model as compared to the fixed prescribed value in the non-N model. The incorporation of leaf Rubisco-N modulated photosynthesis algorithms in the N-coupled model, which interact with other soil-plant N cycling processes as well, had improved the seasonal dynamics of evapotranspiration simulations, particularly during the main growing season.

Simulating soil-N processes is a challenging task. The capability to capture the impacts of short-term extreme weather events, such as early spring drought and extreme summer warming would help in more accurate predictions of soil N processes, such as mineralization, nitrification and denitrification, which largely depend on soil water content and soil temperature. Also, soil freeze and thaw processes simulation may impact N_2O flux simulation during the winter and early spring.

Coupling of nitrogen in the model would help to evaluate nitrogen cycle feedbacks on carbon exchanges in various terrestrial forest ecosystems under future climate change. It would also help to develop forest management strategies to sequester atmospheric carbon dioxide.

REFERENCES

Aber, J. et al., 1998. Nitrogen Saturation in Temperate Forest Ecosystems. BioScience, 48(11): 921-934.

Arain, M.A. et al., 2002. Effects of seasonal and Interannual climate variability on net ecosystem productivity of boreal deciduous and conifer forests. Canadian Journal of Forest Research-Revue Canadienne De Recherche Forestiere, 32(5): 878-891.

Arain, M.A. and Restrepo-Coupe, N., 2005. Net ecosystem production in a temperate pine plantation in southeastern Canada. Agricultural and Forest Meteorology, 128(3-4): 223-241.

Arain, M.A., Yuan, F.M. and Black, T.A., 2006. Soil-plant nitrogen cycling modulated carbon exchanges in a western temperate conifer forest in Canada. Agricultural and Forest Meteorology, 140(1-4): 171-192.

Arain, M.A., Peichl, M., Brodeur, J.J., Restrepo-Coupe, N., Khomik, M. and Mackay, S., 2009. Impact of drought and heat events on seasonal and annual variability of carbon exchanges in an age-sequence of pine forests. Journal of Geophysical Research-Biogeosciences (in review).

Arora, V.K., 2003. Simulating energy and carbon fluxes over winter wheat using coupled land surface and terrestrial ecosystem models. Agricultural and Forest Meteorology, 118(1-2): 21-47.

Arora, V.K. and Boer, G.J., 2003. A representation of variable root distribution in dynamic vegetation models. Earth Interactions, 7: 6-19.

Arora, V.K. and Boer, G.J., 2005a. Fire as an interactive component of dynamic vegetation models. Journal of Geophysical Research-Biogeosciences, 110(G2).

Arora, V.K. and Boer, G.J., 2005b. A parameterization of leaf phenology for the terrestrial ecosystem component of climate models. Global Change Biology, 11(1): 39-59.

Arora, V.K. and Boer, G.J., 2006. Simulating competition and coexistence between plant functional types in a dynamic vegetation model. Earth Interactions, 10.

Billings, S.A., 2008. Nitrous oxide in flux. Nature, 456(7224): 888-889.

Bonan, G., 2008. Carbon cycle: Fertilizing change. Nature Geosci, 1(10): 645-646.

Bonito, G.M., Coleman, D.C., Haines, B.L. and Cabrera, M.L., 2003. Can nitrogen budgets explain differences in soil nitrogen mineralization rates of forest stands along an elevation gradient? Forest Ecology and Management, 176(1-3): 563-574.

Calanca, P. et al., 2007. Simulating the fluxes of CO_2 and N_2O in European grasslands with the Pasture Simulation Model (PaSim). Agriculture, Ecosystems & Environment, 121(1-2): 164-174.

Chapin, F.S.I., Matson, P.A. and Mooney, H.A., 2002. Principles of Terrestrial Ecosystem Ecology. Springer, New York, 436 pp.

Chen, J.M. et al., 2006. Leaf area index measurements at Fluxnet-Canada forest sites. Agricultural and Forest Meteorology, 140(1-4): 257-268.

Ciais, P. et al., 2005. Europe-wide reduction in primary productivity caused by the heat and drought in 2003. Nature, 437(7058): 529-533.

Cox, P.M., Betts, R.A., Jones, C.D., Spall, S.A. and Totterdell, I.J., 2000. Acceleration of global warming due to carbon-cycle feedbacks in a coupled climate model. Nature, 408(6809): 184-187.

Dai, Y., Dickinson, R.E. and Wang, Y.-P., 2004. A Two-Big-Leaf Model for Canopy Temperature, Photosynthesis, and Stomatal Conductance. Journal of Climate, 17(12): 2281-2299.

Davidson, E.A. and Janssens, I.A., 2006. Temperature sensitivity of soil carbon decomposition and feedbacks to climate change. Nature, 440(7081): 165-173.

De Schrijver, A. et al., 2008. Nitrogen saturation and net ecosystem production. Nature, 451 (7180): E1-E1.

Dickinson, R.E. et al., 2002. Nitrogen Controls on Climate Model Evapotranspiration. Journal of Climate, 15(3): 278-295.

Dufresne, J.L. et al., 2002. On the magnitude of positive feedback between future climate change and the carbon cycle. Geophys. Res. Lett., 29.

Environment Canada, 2005. 2004 Canadian acid deposition science assessment: summary of key results. ISBN 0-662-68662-4.

Firestone, M.K. and Davidson, E.A., 1989. Microbiological basis of NO and N_2O production and consumption in soil. Exchange of Trace Gases between Terrestrial Ecosystems and the Atmosphere. Wiley, New York, 7-21 pp.

Flanagan, L.B., 2005. Cross Site Stable Isotope Project.

Fluxnet-Canada, 2004. http://www.fluxnet-canada.ca/

Friedlingstein, P. et al., 2006. Climate-Carbon Cycle Feedback Analysis: Results from the C^4MIP Model Intercomparison. Journal of Climate, 19(14): 3337-3353.

Frolking, S.E. et al., 1998. Comparison of N_2O emissions from soils at three temperate agricultural sites: simulations of year-round measurements by four models. Nutrient Cycling in Agroecosystems 52: 77-105.

Goldberg, S.D. and Gebauer, G., 2009. Drought turns a Central European Norway spruce forest soil from an N_2O source to a transient N_2O sink. Global Change Biology, 15(4): 850-860.

Grant, R.F. et al., 2005. Intercomparison of techniques to model high temperature effects on CO2 and energy exchange in temperate and boreal coniferous forests. Ecological Modelling, 188(2-4): 217-252.

Grant, R.F. et al., 2006. Intercomparison of techniques to model water stress effects on CO2 and energy exchange in temperate and boreal deciduous forests. Ecological Modelling, 196(3-4): 289-312.

Grassi, G., Vicinelli, E., Ponti, F., Cantoni, L. and Magnani, F., 2005. Seasonal and interannual variability of photosynthetic capacity in relation to leaf nitrogen in a deciduous forest plantation in northern Italy. Tree Physiol, 25(3): 349-360.

Grelle, A., Lindroth, A. and Moder, M., 1999. Seasonal variation of boreal forest surface conductance and evaporation. Agricultural and Forest Meteorology, 98-99: 563-578.

Heimann, M. and Reichstein, M., 2008. Terrestrial ecosystem carbon dynamics and climate feedbacks. Nature, 451(7176): 289-292.

Hungate, B.A., Dukes, J.S., Shaw, M.R., Luo, Y. and Field, C.B., 2003. Atmospheric Science: Nitrogen and Climate Change. Science, 302(5650): 1512-1513.

IPCC, 2007. Climate Change 2007: The Physical Science Basis. Contribution of Working Group I to the Fourth Assessment Report of the Intergovernmental Panel on Climate Change. Cambridge University Press, Cambridge.

Janssens, I.A. and Luyssaert, S., 2009. Carbon cycle: Nitrogen's carbon bonus. Nature Geosci, 2(5): 318-319.

Kothavala, Z., Arain, M.A., Black, T.A. and Verseghy, D., 2005. The simulation of energy, water vapor and carbon dioxide fluxes over common crops by the Canadian Land Surface Scheme (CLASS). Agricultural and Forest Meteorology, 133(1-4): 89-108.

Li, C., Aber, J., Stange, F., Butterbach-Bahl, K. and Papen, H., 2000. A process-oriented model of N2O and NO emissions from forest soils: 1. Model development. J. Geophys. Res., 105(D4): 4369-4384.

Magnani, F. et al., 2007. The human footprint in the carbon cycle of temperate and boreal forests. Nature, 447(7146): 849-851.

Nadelhoffer, K.J. et al., 1999. Nitrogen deposition makes a minor contribution to carbon sequestration in temperate forests. Nature, 398(6723): 145-148.

Oechel, W.C. et al., 1994. Transient nature of CO2 fertilization in Arctic tundra. Nature, 371(6497): 500-503.

Parton, W.J. et al., 1996. Generalized model for N_2 and N_2O production from nitrification and denitrification. Global Biogeochemical Cycles, 10(3): 401-412.

Peichl, M. and Arain, M.A., 2006. Above- and belowground ecosystem biomass and carbon pools in an age-sequence of temperate pine plantation forests. Agricultural and Forest Meteorology, 140(1-4): 51-63.

Peichl, M. and Arain, M.A., 2007. Allometry and partitioning of above- and belowground tree biomass in an age-sequence of white pine forests. Forest Ecology and Management, 253(1-3): 68-80.

Peichl, M., Arain, A., Ullah, S. and Moore, T.R., 2009a. Carbon dioxide, methane, and nitrous oxide exchanges in an age-sequence of temperate pine forests. Global Change Biology, (in press).

Peichl, M., Arain, M.A. and Brodeur, J.J., 2009b. Age effects and climatic controls on carbon fluxes in pine forests. Agricultural and Forest Meteorology (in review, accepted with major revision).

Peichl, M., Brodeur, J.J., Khomik, M. and M.A. Arain, 2009c. Biometric and eddy-covariance based estimates of ecosystem carbon exchange in an age-sequence of temperate pine forests. Agricultural and Forest Meteorology, (submitted on June 6, 2009, in review).

Presant, E.W. and Acton, C.J., 1984. The soils of the regional municipality of Haldimand-Norfolk. Volume 1. Report No. 57, Agriculture Canada, Ministry of Agriculture and Food, Guelph, Ontario.

Reay, D.S., Dentener, F., Smith, P., Grace, J. and Feely, R.A., 2008. Global nitrogen deposition and carbon sinks. Nature Geosci, 1(7): 430-437.

Scheffer, M. et al., 2009. Early-warning signals for critical transitions. Nature, 461 (7260): 53-59.

Schimel, D.S. et al., 2001. Recent patterns and mechanisms of carbon exchange by terrestrial ecosystems. Nature, 414(6860): 169-172.

Schlesinger, W.H. and Lichter, J., 2001. Limited carbon storage in soil and litter of experimental forest plots under increased atmospheric CO_2. Nature, 411(6836): 466-469.

Schulze, E.-D., 2000. Carbon and nitrogen cycling in European forest ecosystems Ecological studies, 142. Springer, Berlin. New York 498 pp.

Sokolov, A.P. et al., 2008. Consequences of Considering Carbon-Nitrogen Interactions on the Feedbacks between Climate and the Terrestrial Carbon Cycle. Journal of Climate, 21(15): 3776-3796.

Thornton, P.E. et al., 2009. Carbon-nitrogen interactions regulate climate-carbon cycle feedbacks: results from an atmosphere-ocean general circulation model. Biogeosciences Discuss., 6(2): 3303-3354.

Thornton, P.E., Lamarque, J.-F., Rosenbloom, N.A. and Mahowald, N.M., 2007. Influence of carbon-nitrogen cycle coupling on land model response to CO_2 fertilization and climate variability. Global Biogeochem. Cycles, 21.

Ullah, S. and Moore, T.R., 2009. Soil drainage and vegetation controls of nitrogen transformation rates in forest soils, southern Quebec. J. Geophys. Res., 114.

Verseghy, D., 1991. CLASS--A Canadian Land Surface Scheme for GCMS: I. Soil Model International Journal of Climatology. 11(No. 2): 111-133.

Verseghy, D.L., McFarlane, N.A. and Lazare, M., 1993. CLASS-Canadian land surface scheme for GCMS, II. Vegetation model and coupled runs. International Journal of Climatology, 13(4): 347-370.

Vitousek, P.M. and Howarth, R.W., 1991. Nitrogen limitation on land and in the sea: How can it occur? Biogeochemistry, 13(2): 87-115.

Wang, S., Grant, R.F., Verseghy, D.L. and Black, T.A., 2001. Modelling plant carbon and nitrogen dynamics of a boreal aspen forest in CLASS -- the Canadian Land Surface Scheme. Ecological Modelling, 142(1-2): 135-154.

Warren, C.R. and Adams, M.A., 2001. Distribution of N, Rubisco and photosynthesis in Pinus pinaster and acclimation to light. Plant Cell Environment, 24(6): 597-609.

Wolf, I. and Brumme, R., 2003. Dinitrogen and Nitrous Oxide Formation in Beech Forest Floor and Mineral Soils. Soil Sci Soc Am J, 67(6): 1862-1868.

Yuan, F. et al., 2008. Modeling analysis of primary controls on net ecosystem productivity of seven boreal and temperate coniferous forests across a continental transect. Global Change Biology, 14(8): 1765-1784.

Yuan, F.M., Arain, M.A., Black, T.A. and Morgenstern, K., 2007. Energy and water exchanges modulated by soil-plant nitrogen cycling in a temperate Pacific Northwest conifer forest. Ecological Modelling, 201(3-4): 331-347.

Zak, D.R. and Grigal, D.F., 1991. Nitrogen mineralization, nitrification and denitrification in upland and wetland ecosystems. Oecologia, 88(2): 189-196.

Appendix A

In the model, the maximum photosynthesis capacity for top canopy leaves ($V_{cmax(0)}$) is prescribed. V_{cmax}, for sunlit and shaded big leaves, is scaled-up from top leaves to canopy as follows:

$$V_{c\max,1} = V_{c\max(0)} \cdot \frac{1 - \exp(-(k_N + k_b)L)}{k_N + k_b} \qquad \text{(sunlit)} \qquad \text{(A1)}$$

$$V_{c\max,2} = V_{c\max(0)} \cdot \{\frac{1 - \exp(-k_N L)}{k_N} - \frac{1 - \exp(-(k_N + k_b)L)}{k_N + k_b}\} \quad \text{(shaded)}$$

where, k_N is the foliar nitrogen content decay coefficient; k_b is the beam radiation extinction coefficient, varying with daytime and adjusted by leaf clumping factor; L is LAI. A temperature response function is applied to Eq. A1, if $V_{cmax(0)}$ is prescribed:

$$f(T_{leaf}) = \frac{T_{\max} - T_{leaf}}{T_{\max} - T_{opt}} \cdot \left(\frac{T_{leaf} - T_{\min}}{T_{opt} - T_{\min}}\right)^{\frac{T_{opt} - T_{\min}}{T_{\max} - T_{opt}}} \qquad \text{(A2)}$$

where T_{leaf} is the leaf temperature, and T_{min}, T_{opt} and T_{max} are the minimum, optimum and maximum temperatures for Rubisco activity, in °C. At the end of each model time step (30-min), net assimilation, A_{net}, is calculated by adding the sunlit and shaded photosynthesis rates, which are weighted according to their fractional cover area. The model assumes that sunlit and shaded leaves have same temperature. The model uses a modified version of the Ball-Woodrow-Berry (Ball et al., 1987) formulation for the calculation of bulk stomatal conductance (G_s), which is sensitive to soil water availability, net assimilation, leaf surface CO_2 concentration, and vapor pressure deficit (Arain et al., 2002).

A non-linear relationship between V_{cmax} and Rubisco-N following observations made by Warren and Adams (2001) is included as:

$$V_{c\max(0)} = V_{c\max}(N_{rub0}) \cdot f(T_{leaf}) \qquad \text{(A3a)}$$

where, $f(T_{leaf})$ represents Rubisco-N activity dependence on leaf temperature (Eq. 2), and, $V_{cmax}(N_{rub0})$ is a function of Rubisco-N content in the top canopy:

$$V_{c\max}(N_{rub0}) = \alpha \cdot [1 - \exp(-1.80 \cdot N_{rub0})] \qquad \text{(A3b)}$$

where, α is the maximum value of V_{cmax} and N_{rub0} is leaf Rubisco-N (g N m^{-2} leaf area) in top canopy, estimated from the total amount of nitrogen in entire canopy as:

$$N_{rub0} = \frac{N_{rub} \cdot Nid}{1 - \exp(-k_n \cdot L)} \qquad \text{(A4)}$$

N_{rub} is the total rubisco-related nitrogen in g N m^{-2} (ground area) in the canopy, Nid is the canopy nitrogen inverse decay distance, k_n is the exponential coefficient for N_{rub} decline from top to bottom canopy. L is LAI greater than 1.0 (Warren and Adams, 2001):

$$Na = Na_{\min} + Na_0 \exp(-k_{Na} \cdot L) \qquad \text{(A5)}$$

where Na is Rubisco-N or total nitrogen along the canopy profile used to derive fraction of N_{rub} for Eq. 4, Na_{min} denotes the minimum Na in the bottom canopy, Na_0 is an empirical constant related to the maximum Na, and constant k_{Na} describes nitrogen decline within canopy, i.e. LAI (L).

In the model, nitrogen uptake is calculated as:

$$Nuptake = k_{m0} \cdot \min(\lambda_r, \lambda_t) \qquad \text{(A6)}$$

where k_{m0} is the maximum root uptake rate at reference conditions; λr is ion uptake rate at the root interface; λt is ion transportation rate from bulk to root interface (Dickinson et al., 2002). N_{uptake} can not exceed ($N_{demand} + \Delta N_{pool}$), where N_{demand} is the nitrogen requirement for plant growth, production of ideal N:C ratios, and NPP allocations in leaf, sapwood and fine root. ΔN_{pool} is maximum nitrogen content held in the non-structural pool.

The nutrient ions' (NH_4^+ and NO_3^-) diffusion and transportation from the soil to near root interface (λ_t), which is mainly driven by plant evapotranspiration, and the ions' subsequent absorption through the root interface (λ_r), and the ion concentration at the root surface, is calculated as:

$$\lambda_r = h_p \cdot \frac{C_{fr}}{C_0} \cdot \frac{I_{max}/N_m + K_I}{1 + K_m/N_m} \tag{A7a}$$

where C_{fr} is fine root carbon, C_0 is a reference value for fine root, N_m is ion concentration normalized by 1.0 g m^{-2}, I_{max} (=1.0), K_I (=0.2) and K_m (=0.4) are three non-dimensional root physiological parameters; and h_p represents the reduction of root uptake in a light-limited canopy (Dickinson et al., 2002); and

$$\lambda_t = 0.4 \cdot \frac{W_{rt}}{\rho_{rt}} \cdot \frac{C_{fr}}{C_0} + 0.2 \cdot ET/(ET_0 \cdot \frac{W_{rt}}{\rho_{rt}}) \tag{A7b}$$

where W_{rt} is root zone soil moisture, ρ_{rt} is root zone soil porosity, ET is canopy evapotranspiration, and ET_0 is a reference value of ET. The total nitrogen ion transportation is sum of two inorganic forms, calculated separately, because both are available to plants.

The nitrogen demand for proper plant growth represents nitrogen requirements for converting assimilates into structural tissues and is defined as:

$$N_{demand} = NPP_{lf} \cdot NC_{lf} \cdot 1.25 + NPP_{rt} \cdot NC_{fr} + NPP_{sw} \cdot NC_{sw} + \Delta Nd \tag{A7c}$$

where NPP_{lf}, NPP_{rt}, NPP_{sw} are NPP (net primary production) allocation to leaf, root and sapwood (stem), respectively; and NC_{lf}, NC_{fr}, NC_{sw} are the respective maximum C/N ratios of leaf, fine root and sapwood (for trees, or stem for other vegetations) without nutrient (e.g. N) limitation; and ΔN_d is the nitrogen deficit in the plant, indicating that the plant can absorb more nutrients in order to compensate for a previous deficit (depending on maximum C/N ratios), if available. The factor 1.25 accounts for the fact that leaves can store 25% more nitrogen than their requirement. In the model, when soil nitrogen supplies (λ_r and

λ_t) are not sufficient to satisfy plant nitrogen requirement, and plant experiences nitrogen deficiency, nitrogen allocation to leaves gets first priority and nitrogen in the non-structural pool could also be allocated to leaves.

After the actual nitrogen uptake is estimated, it is then distributed into each of the plant structural pools by their requirements and the rest is allocated to the non-structural pool. The actual nitrogen content in each plant pool is then updated with the current uptake, after litter fall (ΔN_{lt}) and harvesting (ΔN_{har}):

$$\Delta N_{lt} = (1 - frea) \cdot C_{lt\_lf} \cdot NC_{lf} + (1 - frea) \cdot C_{lt\_rt} \cdot NC_{rt} + C_{lt\_st} \cdot NC_{st} \qquad (A8a)$$

where C_{lt_lf}, C_{lt_rt} and C_{lt_st} are carbon losses/turnover from leaf, root and stem, respectively, prescribed in the model; NC_{lf}, NC_{rt}, NC_{st} are described above; and *frea* is fraction of nitrogen reallocation from old tissues to new ones, when carbon turnover/losses occur; and,

$$\Delta N_{har} = C_{hr\_lf} \cdot NC_{lf} + C_{hr\_rt} \cdot NC_{rt} + C_{hr\_st} \cdot NC_{st} \qquad (A8b)$$

where C_{hr_lf}, C_{hr_rt} and C_{hr_st} are carbon losses from leaf and root and stem harvesting, respectively, which are prescribed in the coupled model.

Simulated heterotrophic respiration (R_h) is the sum of CO_2 release from the surface litter layer and the two SOM pools (short-lived and stable), which are influenced by the temperature and soil moisture of the upper 10 and 25 cm soil layers in the model. Litter fall from above-ground plant components contributes to the surface litter pool and that from plant roots contributes to the soil litter pools. R_h is a first-order function of organic C per unit ground area, with a temperature sensitivity defined by a Q_{10} coefficient using the upper (10 cm or 25 cm) soil layer temperatures and water contents (Drewitt et al., 2002):

$$R_h = \sum R_{s0} \cdot C_s \cdot fs(T_s) \cdot fs(\theta_s) \qquad (A9)$$

where, R_{s0} is base respiration rate at reference temperature, C_s represents C pool (litter, short-lived SOM, and stable SOM), $fs(T_s)$ is a Q_{10} soil temperature

function, $fs(\theta_s)$ is a soil moisture function for two SOM pools as described in Bunnell et al.(1977).

Litter respiration is described similarly to Rh, but without the sensitivity to water content. While litter is being decomposed to release CO_2 into atmosphere (R_{slt}), a small fraction of this litter is assumed to humify into two SOM groups at the rate of 0.10 R_{slt} and 0.15 R_{slt} for short-lived and stable SOM pool, respectively. Then assuming that soil biota would eventually stabilize C/N ratio in the stable SOM, the transformation of C from the stable to the short-lived SOM ($C_{som->fom}$) is estimated as:

$$C_{som->fom} = (0.15 \cdot R_{slt} \cdot NC_{lt} - R_{ssom} \cdot NC_{som}) / NC_{som} \qquad (A10)$$

where, NC_{lt} and NC_{som} are actual C/N ratios in litter and stable SOM, R_{slt} and R_{ssom} are respiration rates for litter and stable SOM pools as calculated by Eq. (A12).

Besides leaf-fall, there are three other sources of inorganic nitrogen added to the soil-plant ecosystem: bio-fixation, atmospheric deposition and fertilization. Bio-fixation input, is a function of vegetation coverage, excess soil nitrate, plant structural C pools and environmental temperature (Dickinson et al., 2002):

$$\Delta N_{bf} = S_{bf} \cdot \sigma_f \cdot (1 - fp) \cdot f(T) \cdot \exp(-\beta_f \cdot NO_3^-) \qquad (A11)$$

where S_{bf} is the prescribed reference biofixation rate, σ_f is fraction of vegetation, and fp is the fraction of assimilate to reservoir pool, $f(T)$ is Q_{10} temperature dependence, and β_f is a factor for feedbacks to excess soil nitrate.

Additionally, ammonium volatilization could occur, if prescribed soil pH is greater than 7:

$$-\Delta NH_4^+ = k_v \cdot NH_4^+ \qquad (A12)$$

where k_v is a prescribed volatilization rate.
And drainage occurs as:

$$-\Delta NO_3^- = D_{drainage} / W_{rt} \cdot NO_3^- \qquad\qquad (A13)$$

where $D_{drainage}$ represents water drainage from soil root zone. Otherwise, all NH_4^+ and NO_3^- ions are available for plant root uptakes, as described above.